Republic of Iraq

Ministry of Higher Education and Scientific Research

University of Babylon

College of Science

Department of Physics

Effect of Silica Nanoparticles on Structural and Optical Properties of UHMWPEO/Cu/Ag Nano Composite

A Thesis Submitted to the Council of Physics /College of Science / University of Babylon in Partial Fulfillment of the Requirements for the Degree of Master of Science in Physics

By

Wael Abdulkadhim Atiyah Abd

B.Sc. of Physics /2012

Supervised by

Prof. Dr.

Abdulazeez O. Mousa Al-Ogaili

Prof. Dr.

Mohammed Hadi Shinen Alshammeri

2023 A.D. 1445 A.H.

جمهورية العراق
وزارة التعليم العالي والبحث العلمي
جامعة بابل
كلية العلوم
قسم الفيزياء

تأثير جسيمات السيليكا النانوية على الخصائص التركيبية والبصرية لمتراكب UHMWPEO/Cu/Ag النانوي

رسالة مقدمة إلى مجلس قسم الفيزياء- كلية العلوم - جامعة بابل وهي جزء من متطلبات نيل درجة الماجستير في العلوم/الفيزياء

من قبل

وائل عبد الكاظم عطية عبد
بكالوريوس علوم فيزياء / ٢٠١٢

إشراف

الأستاذ الدكتور
عبد العزيز عبيد موسى العكيلي

الاستاذ الدكتور
محمد هـــــادي شـــنـــين الشمري

١٤٤٥هـ

٢٠٢٣م

الخلاصة

تضمنت هذه الدراسة معرفة تأثير جزيئات السيليكا النانوية على الخواص التركيبية والبصرية للمتراكب المكون من البولي اثلين اوكسايد عالي الوزن الجزيئي وجسيمات النحاس النانوية وجسيمات الفضة النانوية ، وتم تحضير المتراكب UHMWPEO / CuNPs / AgNPs. بعد ذلك تمت إضافة جزيئات السيليكا النانوية بنسب وزنية (0.05 , 0.07 و 0.09) لتكوين متراكب نانوي UHMWPEO / Cu / Ag: SiO_2. تم خلط المكونات بجهاز دوار عند درجة حرارة الغرفة (30 ± 5) درجة مئوية لمدة ساعتين حتى تحقق التجانس الكامل. باستخدام طريقة الصب ، تمت عملية صب المكونات في طبق بتري بقطر (9) سم وترك الخليط لمدة (10) أيام حتى يجف تمامًا.

تمت دراسة الخصائص التركيبية للافلام الناتجة من خلال تحليل الخواص التركيبية باستخدام تقنية التحليل الطيفي (FTIR) ، وأثبتت الاختبارات التشخيصية أن نوع التفاعل بين مكونات المتراكب هو تفاعل فيزيائي ، تم وصف المتراكب من خلال معرفة المجاميع الوظيفية لإثبات هوية العناصر.

كما تم فحص الأفلام الناتجة عن طريق التحليل الطيفي للأشعة السينية المشتتة للطاقة (EDX) لتحليل تكوين العناصر وإثبات نقاوتها ، حيث كانت العينة الأولى خالية من جزيئات السيليكا النانوية ، بينما أظهرت العينة الأخرى جزيئات السيليكا النانوية ، وهذا يثبت نقاء العناصر المكونة.

تم فحص الأفلام الناتجة عن طريق المجهر الإلكتروني للانبعاثات الميدانية لتتبع توزيع وانتشار المكونات المركبة قبل وبعد إضافة جزيئات السيليكا النانوية. نلاحظ أنه تم الحفاظ على تجانس المتراكب وتم منع التكتلات أو التشققات في مكونات الافلام الناتجة مع زيادة الحجم الحبيبي حيث يبدأ من (35.7) نانومتر دون إضافة جزيئات السيليكا النانوية ، وينتهي في (54.2) نانومتر مع إضافة النسبة الوزنية (0.09) من جزيئات السيليكا النانوية. كما ظهرت أشكال مختلفة مع اختلاف التراكيز لجزيئات السيليكا النانوية ، بما في ذلك الأشكال الكروية والزهرية والأشكال الأخرى.

اما نتائج فحص الأفلام الناتجة من استخدام حيود الأشعة السينية (XRD). وجد أن هناك نمو واضح في الجسيمات النانوية يبدأ من (30.06) نانومتر لبلورات المتراكب بدون جزيئات السيليكا النانوية وتستمر في الزيادة حتى تصل إلى (37.12) نانومتر مع جسيمات السيليكا النانوية مما أدى إلى زيادة حجم البلورات.

تم دراسة الخواص البصرية مثل الامتصاصية والانعكاسية والمعاملات البصرية ، فقد زادت جميعها مع زيادة نسب الوزن لجسيمات السيليكا النانوية. أما النفاذية وفجوة الطاقة فقد انخفضت وقد سجلت فجوة الطاقة انخفاض من (3.95) الكترون فولت إلى (3.78) الكترون فولت وتشير هذه النتائج إلى تحسن في جميع المعاملات الضوئية التي تم ذكرها.

Summary

This study included the effect of silica nanoparticles on the structural and optical properties of a composite consisting of ultra-high molecular weight polyethylene oxide, copper nanoparticles and silver nanoparticles, the UHMWPEO /CuNPs/ AgNPs composite was prepared. Silica nanoparticles were added in percentages by (0.05, 0.07 and 0.09)wt% to form a UHMWPEO /Cu/Ag:SiO_2 composite. The ingredients were mixed is that magnetic stirrer at room temperature (30 ± 5) °C for two hours until complete homogenization. Using the casting method, the process of pouring the matrix into a petri dish with a diameter of 9 cm was done and the solution was left for 10 days until it was completely dry.

The structural properties of the films were studied by analyzing the structural properties using Fourier Transform Infrared Spectroscopy (FTIR), the diagnostic tests proved that the type of interaction between the components of the nano composite is a physical interaction, and the functional groups of the components of the superimposed were described by knowing the functional aggregates to prove the purity of the elements.

The resulting films were also examined by energy dispersive X-ray spectroscopy (EDX) to analyze the composition of the elements and prove their purity, as the first sample was free of silica nanoparticles, while the other sample showed silica nanoparticles, and this proves the purity of the constituent elements.

The resulting films were examined by field emission scanning electron microscopy (FESEM) to track the distribution and diffusion of the composite components before and after the addition of the silica nanoparticles. We note that the homogeneity of the overlay was maintained and agglomerations or cracks were prevented in the components of the resulting films with an increase in the grains size starts from (35.7)nm without adding silica nanoparticles, and ends in (54.2)nm with the addition of (0.09) wt% silica nanoparticles. Various shapes were obtained, including spherical, flower and other shapes.

The resulting films were also examined using X-ray diffraction (XRD). It was found that there is a clear growth in nanoparticles starting from (30.06) nm for superimposed crystals without silica nanoparticles and continuing to increase until it reached (37.12) nm which led to an increase in the size of the crystals, as well as relaxation in the nature of the superimposed materials.

As for the optical properties such as absorbance, reflectivity, and optical coefficients, all of them increased with the increase in the weight ratios of the silica nanoparticles. As for the transmittance and energy gap, they decreased from (3.95) eV to (3.78) eV. These results indicate an improvement in all the optical coefficients that were mentioned.

بِسْمِ اللَّهِ الرَّحْمَنِ الرَّحِيمِ

((قَالُوا سُبْحَانَكَ لَا عِلْمَ لَنَا إِلَّا مَا عَلَّمْتَنَا ﷺ إِنَّكَ أَنتَ الْعَلِيمُ الْحَكِيمُ))

صَدَقَ اللهُ العَلِيُّ العَظيم

سورة البقرة

الاية (٣٢)

ACKNOWLEDGMENTS

First of all, my deepest gratitude goes to ALLAH (the Almighty)

the compassionate, and the merciful for everything.

I would like to enlarge my thanks and gratitude to

my supervisors

Prof. Dr. Abdulazeez O. Mousa Al-Ogaili

and

Prof. Dr. Mohammed Hadi Shinen alshammeri

for remarkable notes during the whole of mine.

Many thanks to

the Deanery of the College of Science in Babylon University and the Department of Physics for giving me the chance to complete my study.

I am very grateful to Dr. Karar Abdali O. for his help me throughout

the research work.

Thanks to all my physics department teams and colleagues

who supported me during my academic career

Wael

Dedication

To whom I wish they would share with me the fruit of my effort

but God's will is greater than my wishes

(my father and mother, may God have mercy on them)

To the one who sacrificed his life for the sake of the homeland, the heroic martyr

(my brother Razaq)

To my brothers and sisters, my support in my life

To my dear, beloved, and companion (my wife)

To my children (Somana and Saif), they were a source of light on my path

To everyone who supported and encouraged me in my life and gave me a push forward

Wael

1.1 Introduction

In recent years, the use of most polymers was limited to the manufacture of cheap products which were used for simple purposes. However, the speedy technical development has required the replacement of some materials being used in industry with others having better specifications, consequently, polymers have replaced iron and aluminum for some purposes that require high temperature and stress [1].

Polymer composites have unrivaled properties like light weight, high flexibility, and possibility to be produced at low temperature and low cost [2]. The polymers can be divided into two denominations: industrial and natural. The natural polymers include proteins, cellulose, starches and rubber, either the industrial polymers include poly(vinyl chloride), polypropylene, nylons polyethylene, polyvinyl alcohol, polyacrylamide and polyesters poly carbonate etc.[3].

Over the past few years, a little word with big potential has been rapidly insinuating itself into the world's consciousness, that word is "Nano". Nanotechnology is one of the leading scientific fields today since it combines knowledge from the fields of physics, chemistry, biology, medicine, informatics, and engineering. It is an emerging technological field with great potential to lead in great breakthroughs that can be applied in real life. Nanotechnology tools and techniques enable the fabrication and control of new nano and biomaterials, as well as nanodevices [4].

Nanotechnology, often known as nanoscale science, is the study of matter at the nanoscale, which is defined as the range of (1 to 100) nm. A breakthrough in academic and industrial interest in these nanomaterials over

the past 10 years has been of interest due to the remarkable differences in solid-state properties. In Greek, "Nano" means little man, while the SI unit "Nano" corresponds to (10^{-9} m) magnitudes, such as nanometers, nanoliters, nanograms [5].

The nanosciences have attracted a lot of interest for a number of reasons. Among them, the very large surface to volume ratio showed by many nanoscaled materials opened novel possibilities in surface-based science, such as heterogeneous catalysis [6].

Moreover, it has been discovered that the properties of materials change as their size approaches the nanoscale, or when a portion of certain atoms on the material's surface becomes significant. For example, inert metals such as platinum can act as catalysts, semiconductors such as silicon can act as conductors that become conductive, etc. The applications of nanotechnology have only increased in recent years, and the highest potential application is in the field of materials, followed by electronics and medicine [7].

1.2 Polymer Structure

Polymers are large organic molecules (macromolecules) composed of small structural components (monomers) linked together in a polymerization process [8]. Each molecule is made up of thousands of atoms that are connected by covalent chemical bonds, and molecules in polymers are attracted to one another by forces that vary depending on the polymer type. Polymers with low temperatures have limited crystal connections because polymers are made up of big, linked molecules that are difficult to handle. A linear chain of molecules can only arrange itself in an orderly fashion in a few

locations. In the solid state, polymers have crystalline and non-crystalline regions [9].

1.3 Classification of Polymers

Polymers can be classified into different categories based on their structure, properties, applications, etc . Here are some of the common classifications of polymers.

There are different kinds of polymers categorized according to their structure, and as follows [10].

1.3.1 Linear Polymers

Single molecular is the basic structural unit for polymers in a series of certain lengths that are connected in a linear form. Linear polymers may include totals twisted that are a part of monomer but without any branch, as revealed in Figure (1.1a). Such as polyethylene oxide.

1.3.2 Branched Polymers

This type of polymers consists of several branches that could be a Ladder and Crusader or Comb, which is usually present with various lengths, as illustrated in Figure (1.1 b). Such as low density polyethylene.

1.3.3 Cross Linked Polymers

This kind of polymers consists of chains from three dimensional linked together in more than one site and monomers bonding in effective totals that are chemical bonds, as displayed in Figure (1.1 c). Such as polyvinyl chloride.

1.3.4 Network polymers

Three-dimensional (3D) networks are made of trifunctional. Examples: phenol-formaldehyde and epoxies, as in the Figure (1.1d). Such as nylon.

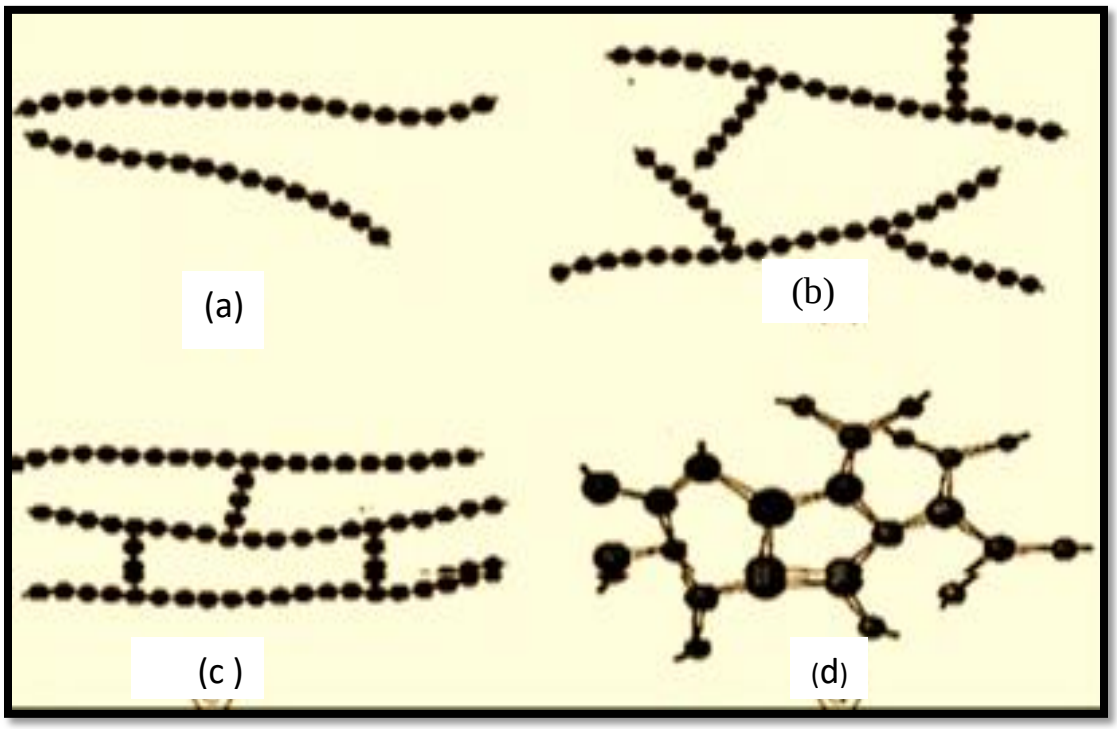

Figure (1.1): Polymeric Chains Types (a) Linear, (b) Branched, (c) Cross-Linked and (d) Network Polymers [11].

1.4 Nanomaterials

Over the past century, the branch of nanotechnology has greatly blossomed. Today, many types of research are directly or indirectly related to nanotechnology. Nanotechnology can be categorized as the development, synthesis, characterization, and application of materials and devices by modifying their size and shape at the nanoscale. The prefix nano is employed as a keyword in every flow, including product advertising. Nano

is a combination of physics, chemistry, materials science, solid-state, and biological sciences, and is derived from the Greek wordnanosor Latin wordnanus, which meaning "dwarf," as a result, mastery in a single subject will not enough. Therefore, physics, chemistry, materials science, solid-state physics [12].

Nanotechnology has a wide range of applications in science and technology. The difference between nanoscience and nanotechnology is that nanoscience is concerned with the arrangement of atoms and their fundamental properties at the nanoscale level, whereas nanotechnology is concerned with the technology used to administer matter at the atomic level for the synthesis of new nanomaterials with various properties [13]. Nanotechnology is intriguing. Although the general public is unaware of its existence in practically all disciplines of engineering, its broad application in medicine, the environment, electronics, defense, and security is still growing. Although a lot of work has been done using this technology, there is still room for the development of new nanomaterials in various fields for the advancement of mankind [12].

Nanomaterials have applications in the field of nano technology, and displays different physical chemical characteristics from normal chemicals (i.e., silver nano, carbon nanotube, fullerene, carbon nano).

According to the classification, nanostructured materials are classified as zero dimensional, one dimensional, two dimensional and three dimensional nanostructures , as shown in Figure (1.2) [14].

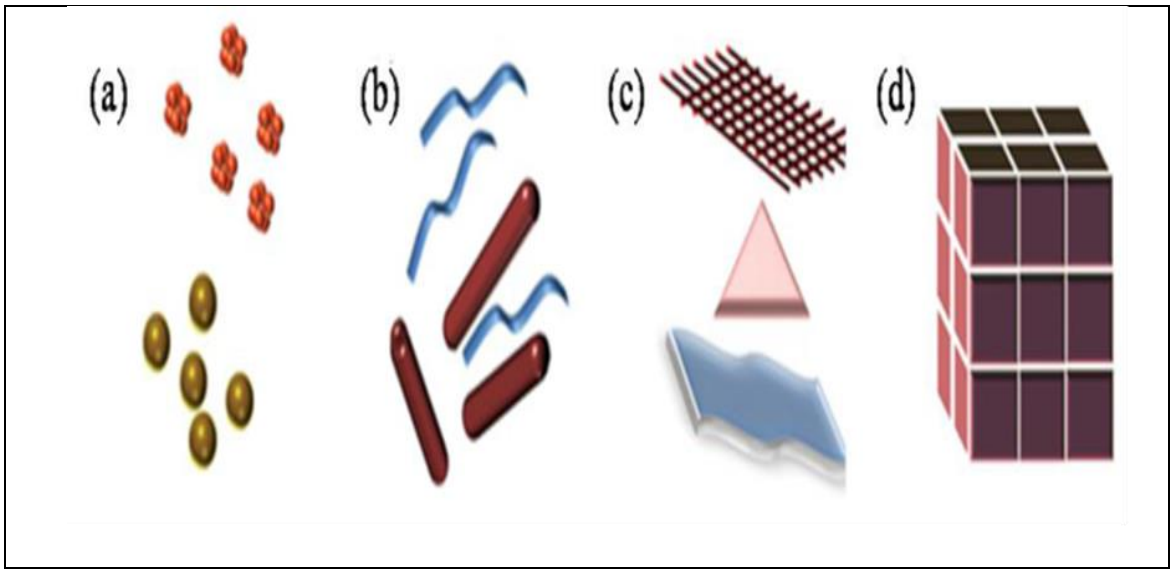

Fig. (1.2): Classification of Nanomaterials (a) 0D Spheres and Clusters, (b) 1D Nanofibers, Wires, and Rods, (c) 2D Films, Plates, and Networks, (d) 3D Nanomaterials[14].

Nanomaterials deal with very fine structures: a nanometer is a billionth of a meter. This indeed allows us to think in both the ‘bottom up’ or the ‘top down’ approaches Figure (1.3) to synthesize nanomaterials, i.e. either to assemble atoms together or to disassemble (break, or dissociate) bulk solids into finer pieces until they are constituted of only a few atoms. This domain is a pure example of interdisciplinary work encompassing physics, chemistry, and engineering upto medicine [15].

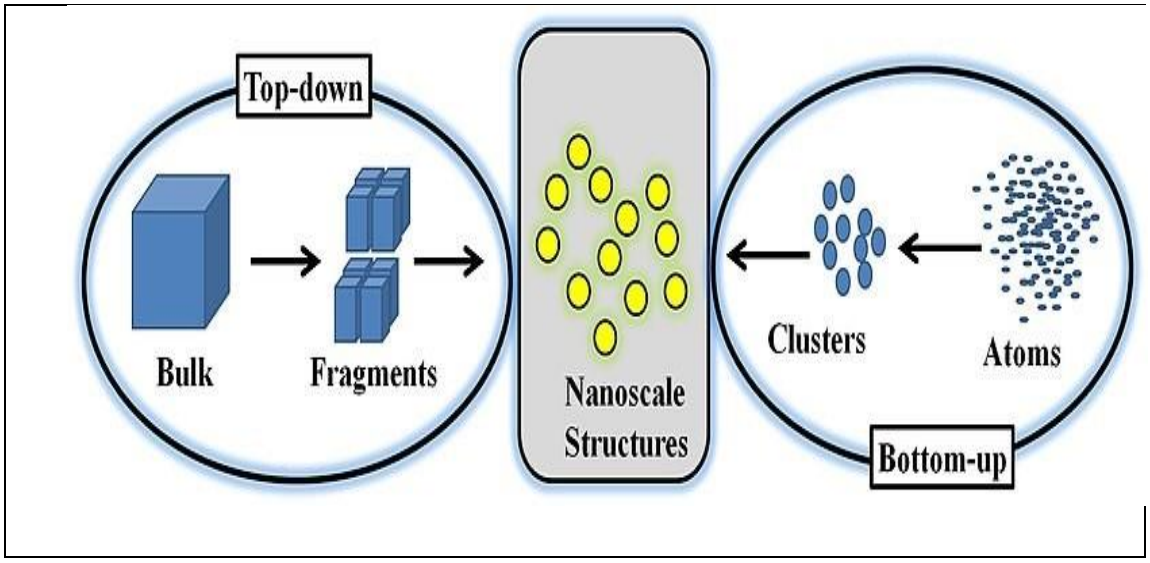

Fig. (1.3): Schematic Illustration of the Preparative Methods of Nanoparticles[15].

1.5 Materials used in the Work

Four different materials were mainly used in this work, three of which are in fixed proportions and the other one is of variable concentration:

1.5.1 Silica Nanoparticle (SiO_2)

Silica is another name for silicon oxides - the most prevalent type being SiO_2. It can be found in nature in crystalline form (as quartz sand), and it is the most abundant component of the earth's crust. Amorphous silica, on the other hand, is industrially manufactured in a variety of forms - including silica gels, precipitated silica, fumed silica, and colloidal silica. Within the construction industry aqueous dispersions of colloidal silica are also referred to as nano silica and used for example in geotechnical, concrete and other concrete applications. The term nano silica can also have a wider definition and include other types of silica in powder form[16].

Silica particles of 1 μm were first prepared using sol-gel method and systematically characterized by Stober and coworkers[16]. Have done extensive work on the preparation of silica nanoparticles ranging from few hundred nanometers to several micrometers by the control hydrolysis of Tetraethyl orthosilicate (TEOS) in ethanol [17].

The size and shape of silica nanoparticles may be controlled by additives such as electrolytes, surfactants and organic acids etc [18,19].

1.5.2 Ultra High Molecular Weight Polyethelen Oxide (UHMWPEO)

UHMWPEO is a high-molecular-weight and non-ionic polymer. It is hydrophilic, linear and not cross-linked, and highly soluble in both aqueous and organic solvents. This repeating unit contains a hydrophobic ethylene group and hydrophilic oxygen, which is also a hydrogen bond site. PEOs are synthesized by polymerization of ethylene oxide using a metallic catalyst. They are available in a very wide molecular weight range, from (200 to 7.0×10^6)g/mol, and the low-molecular-weight PEO are called PEG. They are completely soluble in cold and warm water [20,21].

1.5.3 Copper (Cu NPs)

Copper nanoparticle are elongated nanostructures with an average diameter of(40-100) nm and length of up to 50 μm. Applications for copper nanoparticle include battery technology, microelectronics, solar cells, light-emitting diode (LED) , renewable energy, and medical imaging. Copper nanoparticle are generally available in most volumes, including bulk orders. American elements also manufactures copper nanoparticle dispersions in aqueous and organic solvents such as hexane and ethanol. Copper nanoparticle could have promising applications in electronics [22].

Optoelectronics, solar cells, photonics, magnetics, genetic engineering, chemical sensors, and lubrication, due to their unique characteristics such as high electrical conductivity and thermal conductivity as well as high aspect ratio and tribological properties. Particularly, copper nanowires often can effectively improve the mechanical properties, thermal properties, and wear resistance of polymers such as polystyrene and polyamide [23] .

1.5.4 Silver (Ag NPs)

Silver has a distinctive color that lies between white and gray, which is attributed to it and is said to be silver. It has distinctive properties, as it has the highest value among metals in terms of electrical and thermal conductivity, as well as reflectivity[24].

Silver is found in the earth's crust either in the natural elemental free form, or in the form of an alloy with gold, or within the components of some minerals such as argentite and chlorargerite. Most silver is obtained as a by-product of refining and other metals such as gold, copper and lead. Silver is one of the precious metals as well as from the metals of money, so it was used to mint coins, alone or sometimes with gold. Although it is more abundant in nature than gold, the abundance in the form of the natural metal is few. Silver has many uses, in addition to its use in the field of jewelry, coinage and financial investments, it has applications in the manufacture of solar panels, water purification, electronic industries and chemical industries, in addition to its use in the silverware industry. Silver is purified during the electrolysis of associated metals, where it is obtained as a high-value by-product. For example, during purification, copper is deposited on the cathode in its

production processes, while the silver associated with copper is deposited on the anode[25]

Silver is taken and purified from impurities by treatment with dilute sulfuric acid, rich in oxygen, and then by heating with lime or silica magma; It is then purified again by electrolysis in a solution of nitrate. At present, silver is mostly produced as one of the by-products of purifying copper, lead or zinc metals by electrolysis; Whereas, in the past, purification was based on the heat treatment of ingots of ores containing silver, according to the "Parks process" [26].

1.6 The Methods of Preparation Polymer Films

Methods that can be used to prepare thick and thin films such as [27].

a- Casting Method

To prepare a film in the casting method, a certain amount of polymer material dissolved in a suitable solvent as water. The polymer solution applied to a horizontal rotating disc set at a suitable temperature, to obtain a homogeneous solution, the speed of solvent evaporation must reduce and the preparation time must be long and this method has been used in this study where all polymeric materials were casted in (9 cm) diameter petri dishes. Casting is a process in which molten flows by gravity or other force into a mold where it solidifies in the shape of the mold cavity.

Other techniques that can be used to prepare thin films such as [27].

b- Spin Coating Method.

c- Dip Coating Method.

d- Langmuir- Blodgett (LB) Method.

e- Electrochemical Method. .

1.7 Literature Survey

This section includes previous studies by researchers and the results of their works:

In (2015), Karar Abdali., [28], studied the enhancement of some physical properties of polyethylene glycol by adding some polymeric cellulose derivatives and its applications, the thesis included a study of the physical properties of Polyethylene glycol (PEG 6000) before and after adding some cellulose polymer derivatives. The optical, mechanical and electrical properties of the composite have been studied.

In (2016), Banerjee S. L., ***et al***., [29], studied this investigates a pot synthesis of silver nanoparticles (Ag Nps) using aqueous solution of chitosan-graft-poly(acrylamide) (Cts-g-PAAm) as a reducing agent and polyethylene glycol (PEG) as a stabilizing agent. The as synthesized Ag Nps was characterized by ultra violet-visible (UV-Vis), Fourier transform infrared (FTIR) and X-ray diffraction (XRD) analysis. Field emission scanning electron microscopy (FESEM). The prepared Ag Nps exhibited strong antimicrobial activity against different gram positive bacteria

(Alkaliphilus, Bascill substillis, Lysinibascillus) and gram negative bacteria (Enterobacter aerogenus, vulnificus and Escherichia coli).

In (2017), Ningning Z., ***et al***., [30], studied the novelty of the ideas synthesis and application of copper nanowires and silver nanosheet-coated copper nanowires as nanofillers in several polymers. They found that Cu@Ag nanowires could effectively increase the thermal stability of the PVC matrix composites. Moreover, due to the special morphology and microstructure, the as-prepared Cu@Ag nanowires can effectively improve the mechanical properties and wear resistance of PVC, UHMWPE.

In (2019) , Bangyao H., ***et al.***, [31], studied the effect of Cu, Ag on the microstructure and IMC evolution of sub5–CuAgNi/Cu solder joints and the experimental results indicated that with the increase of Cu and Ag. The researchers concluded that solidus temperature reduced due to the increase of the eutectic.

In (2019), Shujahadeen B. ***et al.***, [32], studied structural, thermal, morphological and optical properties of PEO filled with biosynthesized Ag nanoparticles: New insights to band gap study PEO filled with biosynthesized Ag nanoparticles: New insights to band gap study. In this study a new insight into the study of bandgap is presented. The solution casting technique was used in the current study to prepare polymer composites based on polyethylene oxide (PEO). Correlation relationship was established between the results of the band gap survey and the XRD analysis. The Ag polymer composites involved adding suspended AgNPs at different concentrations to a PEO solution. The PEO:Ag composite films were found to have broad absorption peaks due to the suspended amorphous AgNPs metallic silver

particles, according to the results of the XRD analysis. The FTIR analysis provided conclusive evidence of complexation between AgNPs and the PEO matrix. Then FTIR and XRD. Pure PEO has been found to be associated with conjugated globules. The AgNPs, there was a decrease in globule size, while in 30 ml AgNPs, the globules appeared larger in size. Estimation of the optical band gaps of the membranes required an in-depth investigation of their optical properties.

In (2020), Ragab H. and Rajeh A.,[33], the chemical generation of silver nanoparticles was achieved by reducing the concentration of silver salt. To confirm the existence of nanoparticles, XRD, TEM, and UV–VIS spectrophotometry were used to characterize the Ag NPs. The casting technique contributed to the creation of novel Ag/PAM/PVA nanocomposites films. Analytical tests using XRD and FTIR confirmed the interaction between the polymer blend and the Ag nanoparticles. The FTIR signal intensity variations with increasing dopant concentration imply a rise in the basicity of the major functional groups, indicating the carbonyl group's potential to behave as a powerful electron donor when interacting with the Ag+ cation. The high conductivity accompanied by the high concentration of Ag^{+} was explained in terms of the amorphicity increase. Therefore, these alterations show that these films are highly sensitive to doping, indicating that they are suitable for use in optical and electrical devices.

In (2021), Karar A. ***et al***.,[34], studied the effect of silver nano-particles on structural, optical and electrical properties of casted (polyvinyl alcohol/ polyacrylamide/polyethylene oxide) composites for antibacterial applications by solution casting method. The diffusion of nanoparticles (NPs) in the blends was examined using an optical microscopy and a scanning electron

microscopy (SEM). The aggregation of NPs was clearly visible in the high-weight additives. Optical microscopy, SEM, and FTIR were used to examine the materials. The absorption spectrum records in the wavelength scope (190-1100) nm. The optical parameters directly proportional to Ag nanoparticle additions except for the transmittance and the energy gap were lowered. The optical parameters show that Ag doping clearly effects on the films characteristics, the optical constants enhanced.

In (2021), Qi H. ***et al***.,[35], studied fabrication of Ag containing antibacterial PEO coatings on pure Mg. Antibacterial plasma electrolytic oxidation (PEO) coatings have been fabricated by in-situ incorporation of Ag particles on pure Mg. It was found that the Ag particles have been partly oxidized and incorporated into the layer during coating formation process. Ag containing PEO coatings can strongly inhibit the growth of *S*. aureus and the antibacterial efficiency of the coatings is mainly associated with the Ag concentration in the layer. The antibacterial rate of the coating reaches 99% and is maintained to be stable when sufficient Ag particles (above 1 wt%) are incorporated into the layer.

In (2021), Xinzhen F.***, et al***.,[36], studied the antimicrobial and antiviral behaviors of Ag and Cu nanoparticles (NPs) are well known, and possible mechanisms for their actions, such as released ions, reactive oxygen species (ROS), contact killing, the immunostimulatory effect, and others have been proposed. Ag and Cu NPs, and their derivative NPs, have different antimicrobial capacities and cytotoxicities. Factors, such as size, shape and surface treatment, influence their antimicrobial activities. The biomedical application of antimicrobial Ag and Cu NPs involves coating onto substrates, including textiles, polymers, ceramics, and metals. Because Ag and Cu are

immiscible, synthetic AgCu nanoalloys have different microstructures, which impact their antimicrobial effects. When mixed, the combination of Ag and Cu NPs act synergistically, offering substantially enhanced antimicrobial behavior.

In (2022), Ahed A. K.,[37], studied the synthesis and characterization of PAAm-PEG blend and the effect of Ag, Sb_2O_3 Nanoparticles: Structural and dispersion parameters .This study included the preparation of polymer mixture films by mixing (PAAm-PEG) and adding different amounts of nanomaterial (Sb2O3, Ag) by casting method. Then, Sb_2O_3, (Ag) was added to the solution with different content with the same particle size to form samples. The homogeneity and distribution of (Sb_2O_3, Ag) nanoparticles in PAAm-PEG-Sb_2O_3, Ag films were studied using a light microscope. The optical microscopy images showed a good dispersion of the nanoparticles with some agglomeration.

In (2022), Zainab M. J.,[38], studied of the effect of nanowire on structural and optical properties PVA-PAAm blend. PVA-PAAm:CuNW nanocomposites were prepared by pouring the solution in different thicknesses (120.90) μm and different weight ratios (0.5, 1, 2)wt% of CuNW. The morphological, structural and optical properties as well as the separation coefficients of the nanocomposites were studied. Optical microscope images showed a good distribution of CuNW atoms within the polymeric mixtures of all nanocomposite films. Scanning electron microscopy (SEM) showed a uniform shape revealing a rather smooth surface, and increasing the CuNW ratio in a polymer matrix of PVA-PAAm:CuNW nanocomposites led to changes in the surface morphology and increased roughness.

In (2022) Tian W. ***et al***.,[39], studied the effect of Cu-/Ag-activation on growth and corrosion resistance of electroless plated Ni-film on plasma electrolytic oxidation coating. Cu activation and Ag activation methods have been developed. Field emission scanning electron microscopy was used to characterize the surface morphology and cross-section morphology of films on Cu and Ag-activated coatings. Compared with the Ag doping coating, a thicker, compact and more uniform layer film was formed on the Ag doping coating. Moreover, the results of the electrochemical tests showed that the film coated with the Ag-doped coating offered somewhat the same corrosion resistance as the film coated on the Ag-activated coating, and better than the film on the Cu-doped coating. Hence, the Ag activation method significantly reduces the cost and, ensures the corrosion resistance of the composite coating.

In (2022), Karar A., ***et al***.,[40], studied morphological, optical, electrical characterizations and anti-escherichia coli bacterial efficiency (AECBE) of PVA/PAAm/PEO Polymer Blend Doped with Silver NPs, Silver nanoparticles (AgNPs) were mixed with a polymer mixture to enhance them van granted . A new approach by applying AgNPs in the polymer blend can improve the physical and antibacterial properties.In the loading process, there were different amounts of AgNPs in succession Coated with polyvinyl alcohol (PVA), polyacrylamide (PAAm) and polyethylene oxide(PEO) polymer blend via casting method. The prepared films were characterized by x-ray and optical microscopy (OM), electron microscopy (SEM), Fourier transform infrared (FTIR) and UV / Visible. The OM and SEM images showed that the AgNPs were well dispersed within the polymer mixed with some weak groupings. Visual properties were improved after doping.

In (2023), Ehssan Al.B. ***et al.***,[41], studied the effect of green synthesis bimetallic Ag@SiO_2 core–shell nanoparticles on absorption behavior and electrical properties of PVA-PEO nanocomposites for optoelectronic applications. A green and easy technique for the aggregation of basic (Ag@SiO_2) nanoparticles into the matrix polymer matrix blend. The core nanoparticles were loaded into ultra-high molecular weight polyvinyl alcohol (PVA).Polyethylene oxide blended polymer (UHMW-PEO) for fabrication of novel nanocombined guns (NCFs) using Casting technique. The ultrastructural and optical properties of the membranes were investigated using X-rays fourier transform infrared, visible light microscopy, scanning electron emission Microscopy (FESEM), UV-vis energy dispersive spectrometry / Study of structural, optical and electrical properties and XRD revealed a semi-crystalline nature the degree of crystallinity increased.

In (2023), Camillo L. and Gianfranco R.[42], studied polymer wrapping onto nanoparticles induces the formation of hybrid colloids. The polymers stabilize the nanoparticles on which they are wrapped, avoiding coagulation and unwanted phase separation processes. Circulation gives rise to hybrid colloids, and is useful in applications with vital purposes. The encapsulation efficiency is controlled by different contributions, which stabilize the polymer plugs. They control the properties of the system when surface adsorption of the hosts is undesirable. Calculations based on the proposed approach have been applied to the PEO coating on SiO, silica and nanoparticles.

1.8 Aims of the Work

The goal of the work includes several points, the most important of which are:

1- The main objective of the current study is to develop a new type of film by casting method that can be used in optoelectronic devices.

2- The study focuses on the effect of incorporating silica nanoparticles (SiO_2) and adding them on to a composite composed of UHMWPEO/ CuNPs/AgNPs.

3- The use of the casting method in this work to improve the structural and optical properties of the resulting films, and the development of new materials with improved properties are necessary to meet these demands.

2.1 Introduction

This chapter discusses the theory and mathematical relations used to define some physical properties. These physical properties are generally classified as structural and optical. These relationships are the basis for understanding and characterizing materials. In general, physical properties can be classified into two broad categories, structural and optical. Structural properties refer to the arrangement of atoms or molecules within a material. Some of the important structural properties of materials include crystal structure, lattice parameters, and atomic positions. These properties can be determined using techniques such as X-ray diffraction, neutron diffraction, and electron microscopy[43].

Optical properties refer to the way that materials interact with light. Some of the important optical properties of materials include reflectivity, transmissivity, and refractive index. These properties can be used to understand how light is absorbed, reflected, or transmitted through a material, and can be measured using techniques such as spectrophotometry, ellipsometry, and polarimetry .

In addition to structural and optical properties, materials can also be characterized based on other physical properties such as mechanical, electrical, magnetic, and thermal properties. Each of these properties can be quantified using specific techniques and mathematical relations, allowing scientists and engineers to understand and manipulate the behavior of materials for various applications[43].

2.2 Structural and Morphology Properties

A wide variety of characterization techniques were used to evaluate the material quality of the thin films before using the films in applications. Structural and morphological characterizations are methods used to analyze the physical and chemical properties of materials at the atomic and molecular levels. These techniques are important in many areas of science and engineering, including materials science, chemistry, physics, and nanotechnology [44].

Structural characterization techniques provide information about the arrangement of atoms or molecules within a material. X-ray diffraction, neutron diffraction, and electron diffraction are commonly used techniques for determining the crystal structure of materials. X-ray photoelectron spectroscopy (XPS), Auger electron spectroscopy (AES), and Raman spectroscopy are other techniques that can provide information about the atomic and molecular structure of materials. Morphological characterization techniques, on the other hand, provide information about the shape, size, and surface features of materials. Scanning electron microscopy (SEM) and transmission electron microscopy (TEM) are commonly used techniques for imaging the surfaces and internal structure of materials. Atomic force microscopy (AFM) and scanning tunneling microscopy (STM) are other techniques that can provide high-resolution images of the surface topography of materials [45].

Overall, structural and morphological characterizations are important tools for understanding the properties and behavior of materials at the atomic and molecular scales, which is critical for developing new materials and improving existing ones.

2.2.1 Principles of Fourier Transform Infrared Spectroscopy

Fourier transforms infrared (FTIR) a chemical investigative spectroscopy. This measures the infrared intensity with light wavenumber. The wavenumbers consist of infrared light that are divided into three regions, far-infrared, mid-infrared and near-infrared, which are between (4 ~ 400) cm^{-1}, between (400 ~ 4,000) cm^{-1} and finally, between (4,000 ~ 14,000) cm^{-1}, respectively [46].

Infrared radiation is permitted to pass through a material in FTIR spectroscopy. Some of the infrared radiation is transmitted and some is absorbed by the sample. The resulting spectrum is similar to the sample's molecular fingerprint and contains information about the various chemical groups and chemical bonds present in the sample. Two molecular structures never generate the same infrared spectrum like fingerprints are unique for every person, as shown in Figure (2.1) [46].

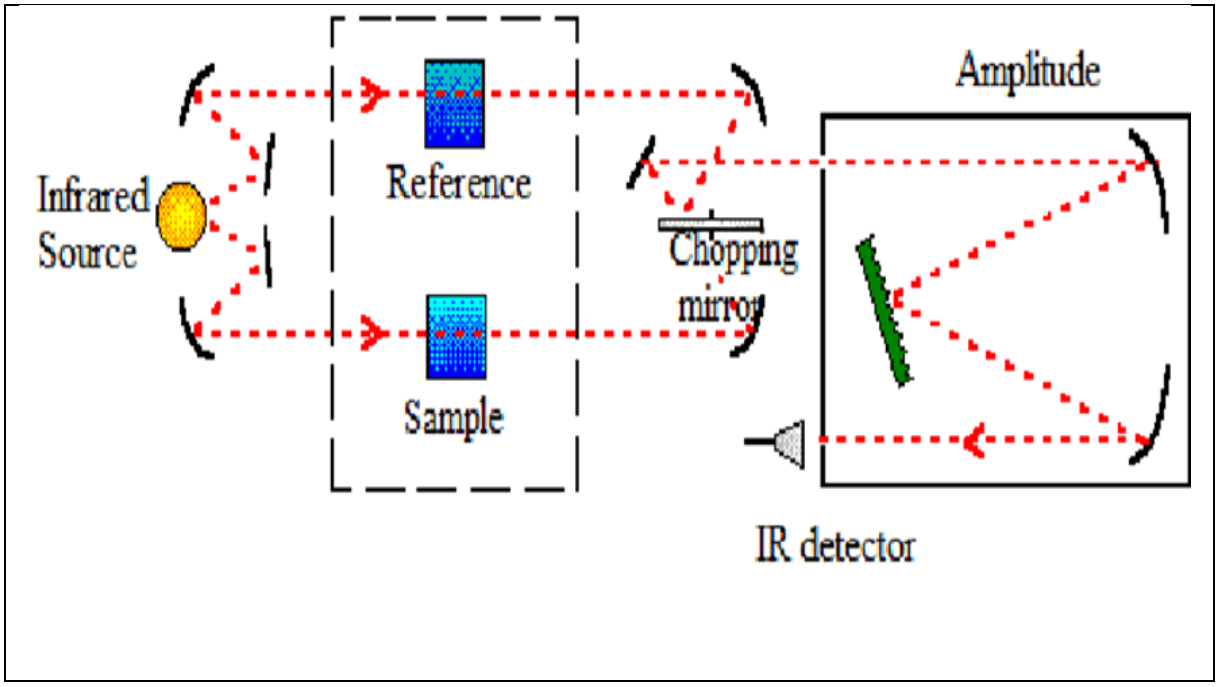

Fig. (2.1): A Schematic Diagram of the Classical Dispersive FTIR Spectrophotometer [46].

2.2.2 Principle of Energy-Dispersive X-ray Spectroscopy

Energy-dispersive X-ray spectroscopy (EDS or EDX) is a technique used in analytical chemistry and materials science to identify and quantify the elemental composition of a sample. EDX is typically performed in conjunction with scanning electron microscopy (SEM), in which an electron beam is focused on a sample and causes the emission of characteristic X-rays from the elements present in sample [47].

EDX works by detecting the energy of the emitted X-rays using a detector placed near the sample. Each element has a unique set of energy levels associated with its electrons, and when an electron transitions from a higher energy level to a lower one, it emits an X-ray with a characteristic energy that is specific to that element. By measuring the energies of the emitted X-rays, EDX can determine the elements present in the sample and their relative abundances, as in Figure(2.2) [48].

EDX is a non-destructive technology that allows analysis of the elemental composition of a sample with high spatial resolution, making it useful for a wide range of applications in materials science, geology, biology, and engineering. However, the accuracy and precision of the EDX depends on a variety of factors, including the quality of the SEM instrument, the sample preparation method, and the calibration of the EDX detector [49].

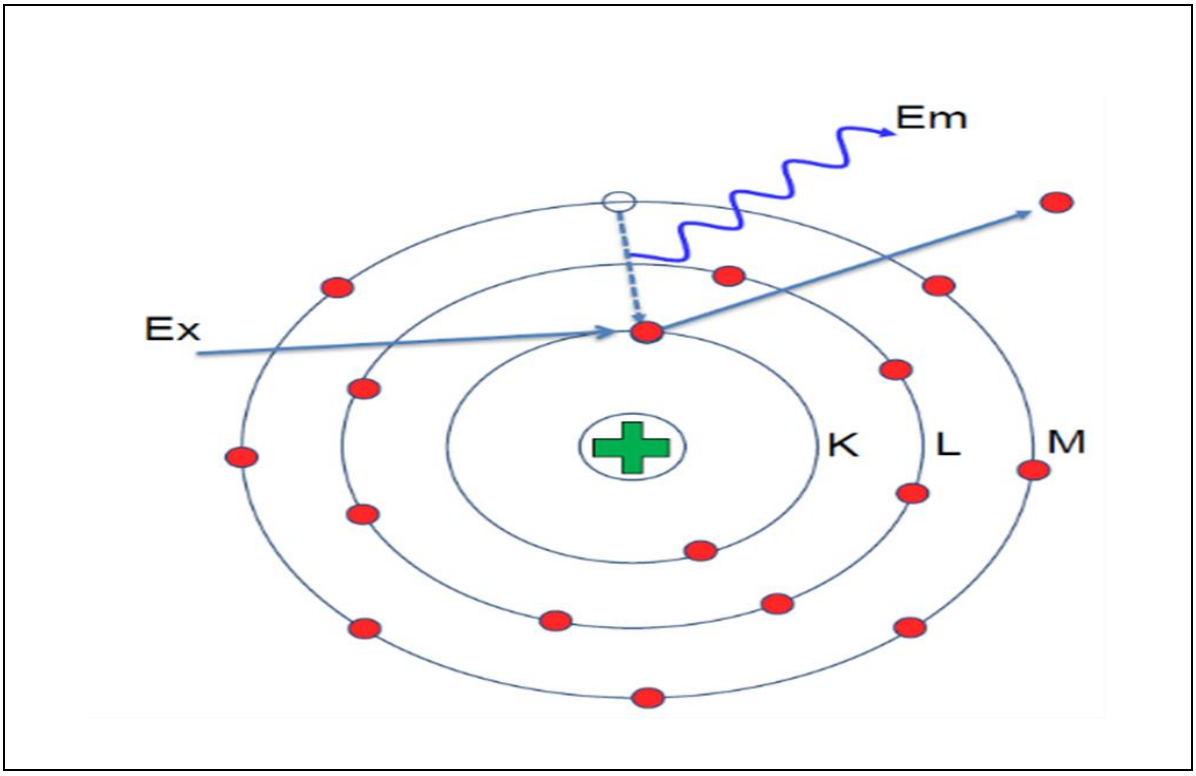

Fig.(2.2): Schematic Diagram of Energy-Dispersive X-ray (EDX)[49] .

2.2.3 Principle of Field Emission Scanning Electron Microscopy

The field emission scanning electron microscopy (FESEM) is a vital research and manufacturing instrument that is widely utilized in many industries throughout the world. The instrument's appeal stems from the necessity to inspect and gather information about samples whose structure is deteriorating.

The FESEM provides a better level of resolution for examination and inspection than existing optical microscope techniques. In addition, unlike the optical microscope, the FESEM has a range of analytical modes, each of which provides unique information on the physical, chemical, and electrical properties of a certain specimen, device, or circuit. Because of recent advances that eliminate or at least minimize sample degradation and contamination, allowing continuous nondestructive

in-process inspection, the FESEM is currently finding increased uses in research and production quality control, as shown in Figure (2.3) [50] .

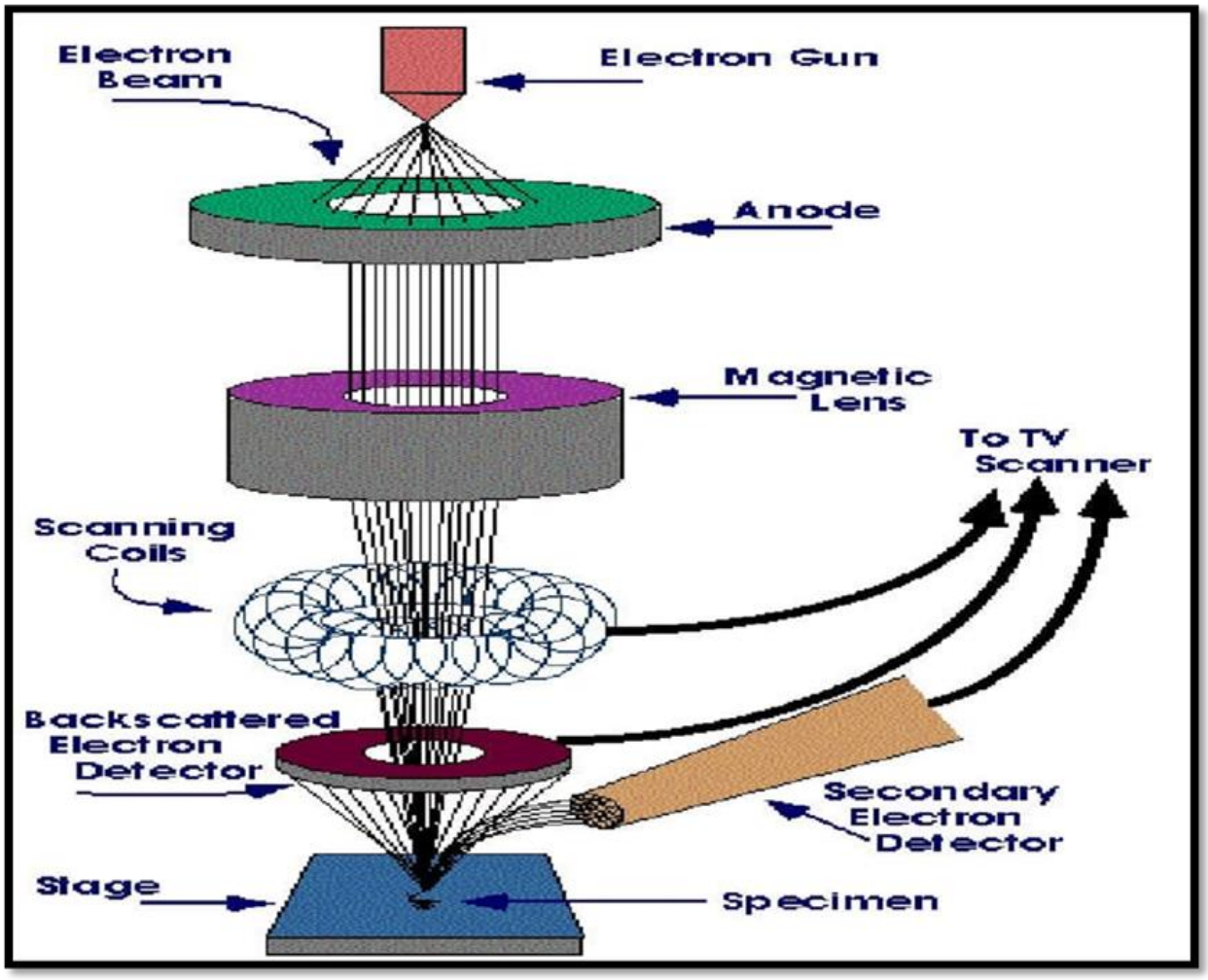

Fig. (2.3): Schematic Diagram of Field Emission Scanning Electron Microscopy (FESEM) [51].

2.2.4 Principle of X-ray Diffraction

X-ray diffraction (XRD) is a powerful technique used to analyze the crystal structure of materials. It works by directing a beam of X-rays onto a crystalline sample, which scatters the X-rays in various directions. The scattered X-rays form a diffraction pattern, which can be analyzed to determine the crystal structure of the sample.

The diffraction pattern results from the interference of X-rays scattered by different planes of atoms in the crystal lattice. By measuring the angles and intensities of the diffracted X-rays, XRD can determine the spacing and orientation of the atomic planes in the crystal lattice, as well as the size and shape of the unit cell that forms the crystal structure. XRD is a non-destructive technique that can be used to analyze a wide range of materials, including minerals, metals, ceramics, and polymers. It is commonly used in materials science, chemistry, geology, and physics to identify unknown crystalline materials, study phase transitions, and investigate the crystal structure of new materials [52].

XRD requires a high-quality X-ray source, such as a synchrotron or an X-ray tube, as well as a high-quality X-ray detector to accurately measure the diffracted X-rays. Sample preparation is also important, as the sample must be finely ground and carefully oriented to produce a high-quality diffraction pattern [52].

The equation and Debye- Scherer equation can be used to indicate the grain size [53].

$$D = (0.9\,\lambda)/(\beta \cos\theta) \qquad (2.1)$$

$$2d_{(hkl)} \sin\theta = n\lambda \qquad (2.2)$$

As :

d: The distance between the two sides' surface.

λ: The length of the wave of the incident ray (1.54 Å).

n: integer (represents order diffractions).

θ: Angle of incidence and reflection of the package X-rays beam and the surface.

(hkl): Millers coefficient

The Bragg reflection is a phenomenon in which X-rays or neutrons are diffracted by the atoms in a crystal lattice in a way that produces a series of constructive interference patterns. This phenomenon was discovered by William Lawrence Bragg and his father William Henry Bragg in 1912 and is named after them. The Bragg reflection occurs when the wavelength of the incident X-rays or neutrons is approximately equal to the spacing between the atomic planes in the crystal lattice. When this condition is met, the X-rays or neutrons are diffracted at a specific angle, known as the Bragg angle, which maximizes the constructive interference between the waves reflected by the atomic planes[54].

The Bragg reflection is an important tool in the study of crystal structures, as it allows scientists to determine the spacing between the atomic planes and the orientation of the crystal lattice. This information can be used to determine the arrangement of atoms within the crystal, which is important for understanding the physical and chemical properties of materials. The Bragg reflection is also used in a variety of other applications, including X-ray diffraction analysis, crystallography, and neutron scattering, this can be illustrated in the Figure(2.4) [55].

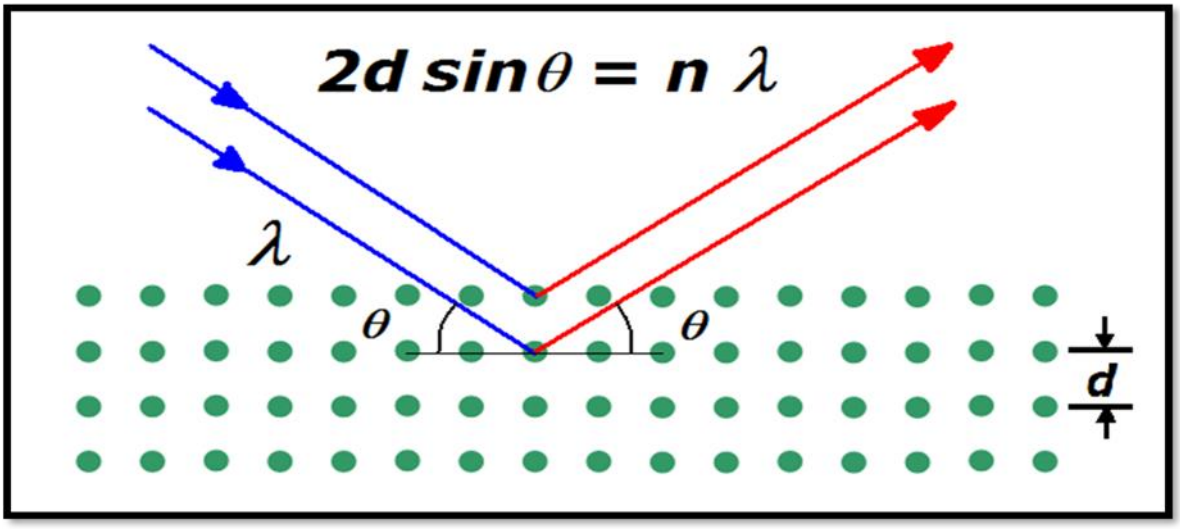

Fig. (2.4): The Bragg Reflection [55].

2.3 Optical Properties

Optical properties of polymers constitute an important aspect in study of electronic transition and the possibility of their application as optical filters, a cover in solar collection, selection surfaces and green house [56]. The optical properties of materials can be defined as any property that involves the interaction between electromagnetic radiation and light with the matter, including absorption, polarization, reflection, and scattering effects .

The optical constants fully describe the optical behavior of materials; they are important and fundamental properties of matter. Knowledge of optical constant of a film from a given material is basic importance in determining the characteristics of light transmission in the film. Such knowledge of the optical parameters of the material is importance when designing devices through which electromagnetic radiation absorbed or transmitted [57].

Study of the optical properties of polymers increases our knowledge of the type of polymer internal structure, nature of the bonds and expands the potential scope of polymer application. Knowing the spectrums of absorption and transmittance of a

polymer assist in identifying many optical properties in different ranges of wavelengths. Conducting examination at the ultraviolet spectrum range enables us to know the type of the bonds, orbital and energy beams. The study at the visible spectrum range provides sufficient information about the behavior of a matter to solar applications. The study at the infrared range is very important in knowing the general structure of a polymer and the elements consisting its chemical structure[58].

The total molecular energy has been broken down into electronic energy (E_{ele}), vibration energy (E_{vib}), rotational energy (E_{rot}) and transitional energy (E_{trans}). Due to the change in the distinct energies, the absorbance of an electromagnetic wave results in a change in the total energy of the molecule [59].

$$\Delta E_{total} = \Delta E_{vib} + \Delta E_{rot} + \Delta E_{ele} + \Delta E_{trans} \qquad (2.3)$$

The visible and ultraviolet spectrums are those of electronic absorbance, while the rest are those of other absorbance. In the absorbance spectrum, the E_{ele} is the clearest. The photon's reaction with the molecule causes the photon's electrical field to agitate the electronic structure of the molecule to the point where The photon vanishes, and its energy is transferred to the molecule whose state has been changed to excited [60]. As shown in Figure (2.5) shows the energy regions and molecular energies.

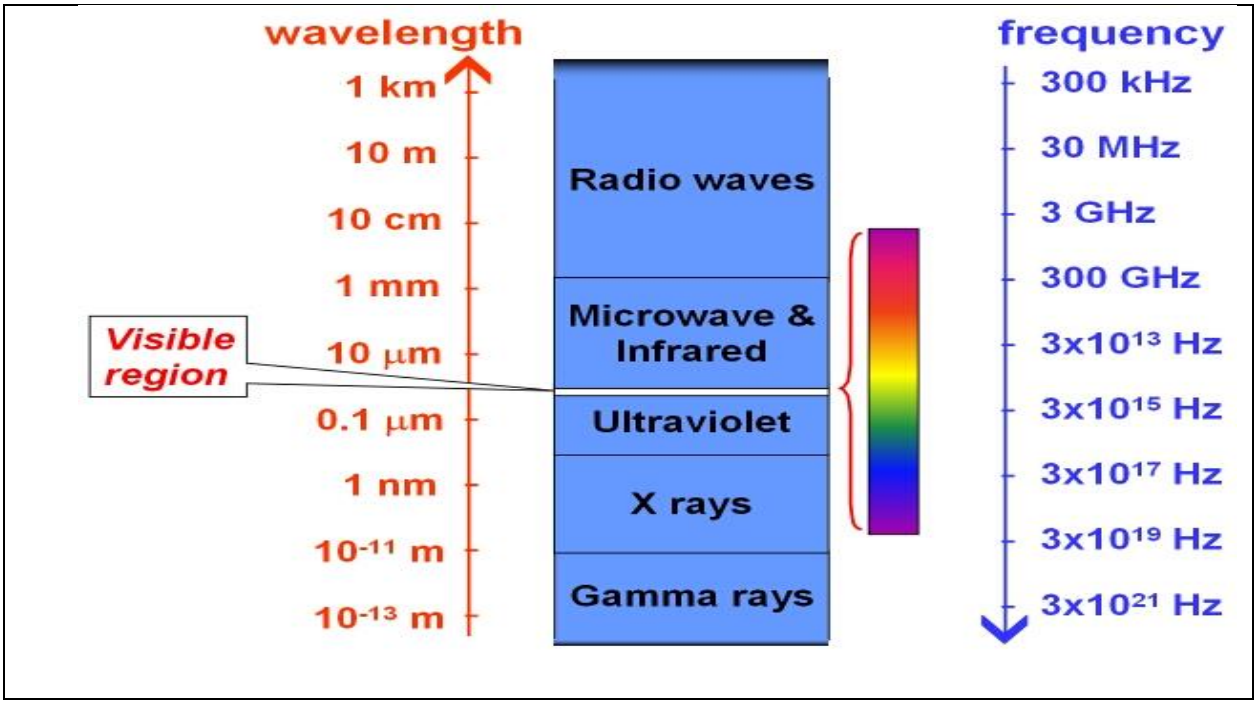

Fig. (2.5): The Electromagnetic Spectrum Region [61].

2.3.1 Reflectivity(R)

Reflectivity can be obtained from absorption and transmission spectrum in accordance to the law of conservation of energy by the relation [62].

$$R+T+A=1 \qquad (2.4)$$

Where:

R: is the reflectance , T: is the transmittance and A: is the absorbance.

2.3.2 Absorbance (A)

The ratio of absorbed light intensity (I_A) by substance to incident light intensity (I_o) is known as absorption [63].

$$A = \log \frac{I}{I_T} \qquad (2.5)$$

2.3.3 Transmittance (T)

Dividing the intensity of the rays transmitting from the film (I_T) over the intensity of the incident rays on it (I_o) is called transmittance (T) and given in equation (2.4) [64].

$$\mathbf{T = \frac{I_T}{I_o}} \qquad \textbf{(2.6)}$$

2.3.4 Optical Constants

There are many ways to find the optical constants of absorption coefficient, refractive index, extinction coefficient and optical conductivity

2.3.4.1 Absorption Coefficient (α)

Absorption coefficient is defined as a ratio decrement in incident ray energy flux relative to distance unit in the direction of incident wave diffusion. The absorption coefficient (α) is determined by incident photon energy (hυ), material characteristics where electronic transitions are type (n) or (p), and forbidden energy gap gives the following equation [65].

$$\mathbf{E = h\upsilon} \qquad \textbf{(2.7)}$$

When incident photon energy is less than the forbidden energy gap, then photon will be transmitted and transmittance gives the following equation [65].

$$\mathbf{T_r = (1 - R)^2 \, . e^{-\alpha t}} \qquad \textbf{(2.8)}$$

If the intensity of incident ray (I_o) that incident on blend film material of thickness (t), the intensity of transmittance ray (I) gives by Beer Lambert law.

$$\mathbf{I = I_0 \, e^{(-\alpha t)}} \qquad \textbf{(2.9)}$$

The absorption coefficient is measured by cm^{-1}.

$$\mathbf{\alpha t = 2.303 \log \frac{I}{I_0}} \qquad \textbf{(2.10)}$$

Where the amount of log (I/I_o) represents the absorbance (A).

The absorption coefficient can be calculated using the following equation: [66].

$$\alpha = 2.303 \left(\frac{A}{t}\right) \qquad (2.11)$$

Where (t) represent a thickness of sample.

2.3.4.2 Refractive Index (n)

It is the ratio of light speed in vacuum to its speed in a medium. This index shows how far a matter is affected by the electromagnetic waves. The refraction index consists of two parts: real and imaginary. It can be expressed by the following equation [64].

$$n = c/v \qquad (2.12)$$

Where (n) is the refractive index , (c) is the light speed in vacuum and (v) is the light speed in matter. Reflectance (R) can also be defined as the ration of the reflected ray relation at the borderline between two mediums to the incident ray.

The relation between reflectivity and refractive index is shown in the following equation [64].

$$R = (n-1)^2 + k_o^2 / (n+1)^2 + k_o^2 \qquad (2.13)$$

Where (k_o) is the extinction coefficient.

The rate of absorption of light is directly proportional to the intensity of the incident light at a specific wavelength, and this physical phenomenon is common and lead to the decay of the light intensity exponential as it passes.

Refractive index can be expressed by the following equation [64].

$$n = [4R/(1-R)^2 - k_o^2]^{1/2} + (R+1)/(R-1) \qquad (2.14)$$

2.3.4.3 Extinction Coefficient (k_o)

The coefficient of inertia represents the amount of photons absorbed by the membrane, that is, the energy absorbed by the electrons of the material, and expresses the following relation [67].

$$k_o = \alpha \lambda / 4\pi \qquad (2.15)$$

Where (λ) is the wavelength of the incident radiation and (α) absorption coefficient.

2.3.5 Absorption Regions

Absorption regions can be classified to three regions :

A) High absorption region: the absorption coefficient value in this area is about ($\alpha \geq 104$ cm-1) and obeys Tauce equation [68].
B) Exponential region: the absorption coefficient value in this area is about runback equation [69].
C) Low absorption region: the absorption coefficient value in this area is about ($\alpha < 10^4$ cm^{-1})) [70].

3.1 Introduction

This chapter is devoted to the experimental part, which plays an important role in determining the results. Where films are prepared (UHMWPEO/Cu NPs/Ag – SiO_2) by casting method. After completing the membrane preparation process, the structural and optical properties of these films were studied. Figure (3.1) shows the schematic diagram of the preparation and characterization.

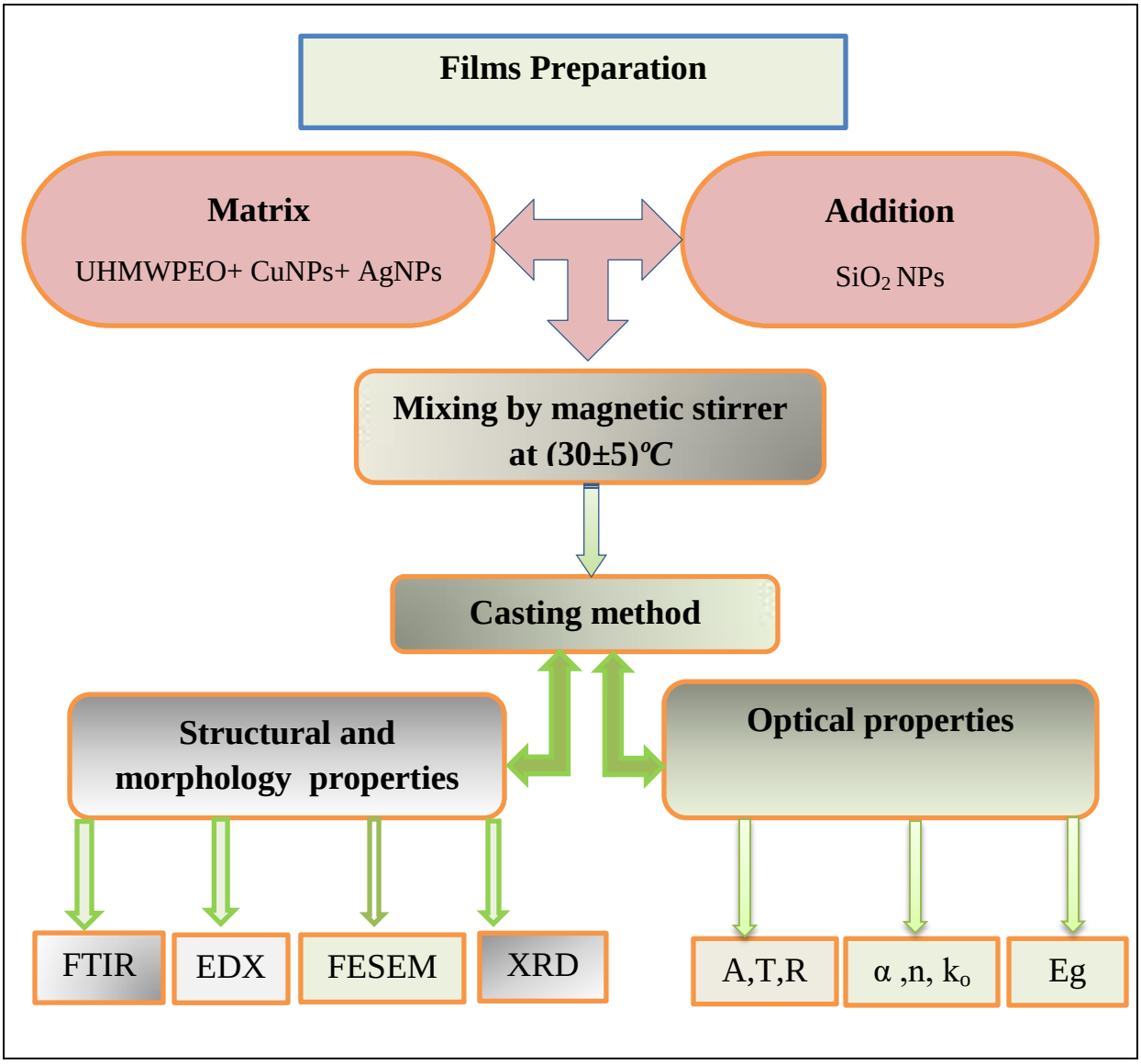

Fig. (3.1): Scheme of Experimental Part.

3.2 Utilized Materials

The mixture used in this work consists of three ingredients:UHMWPEO/Cu NPs/Ag NPs Composite.

3.2. 1 Ultra Higher Molecular Weight Polyethelen Oxide (UHMWPEO)

The polymer was used in a white granular form soluble in distilled water, and its molecular weight was (3×10^6 g/mol), with high purity (99.9%). It manufactured by a company (Central Drug Houses (CDH)).

3.2. 2 Copper Nanoparticles (Cu NPs)

This metal was used with the following specifications, actual particle size APS (30 nm) , purity (99.9%) , specific surface area(15 m^2/g), volume density (0.2 g/cm^3), density (8.9 g/cm^3), particle shape (sphere) and color (brown).

3.2. 3 Silver Nanoparticles (Ag NPs)

The material with an average grain size of 20 to 30 nm and high purity (99.95%), silver nanoparticles (Ag) was produced as a powder by Sky Spring Nano Materials, Lnc.

3.2.4 Silica (NPs)

The addition consists of one material, which is silica nanoparticles, were added in the form of a powder with an actual particle size APS of 20-30 nm, a purity of (99.8%) and a spherical shape. The addition process was carried out in different stages according to the change in the concentrations of nanoparticles of silica with fixed concentrations of the row materials . the thickness of the obtund films where computed using digital micrometer to be in the range between 75µm and 85µm. The applicable concentrations are shown table (3.1).

Table (3.1): Weight Percentages of (PEO/Cu NPs/Ag NPS) Nanocomposite and (SiO_2) NPs.

Matrix materials wt%			Loadings wt%
UHMW PEO	**Cu NPs**	**Ag NPs**	**SiO_2 NPs**
0.96	0.03	0.01	0.00
0.91	0.03	0.01	0.05
0.89	0.03	0.01	0.07
0.87	0.03	0.01	0.09

3.3 Methodology

These techniques have been selected in examination and diagnosis based on the requirements of knowledge of characteristics.

3.3.1 Fourier Transform Infrared Spectroscopy (FTIR)

Fourier Transform Infrared Spectroscopy is another analytical technique used in materials science and chemistry. Measures the absorption or transmission of infrared radiation by a material as a function of wavelength or frequency. By analyzing the resulting spectrum, we can obtain information about the molecular vibrations and functional groups present in the material. In the context of our experiment, FTIR spectroscopy can be used to analyze the chemical composition and structure of the UHMWPEO/Cu NPs/Ag:SiO_2 films.

By measuring the absorption or transmission of infrared radiation at different frequencies, researchers can identify the functional groups present in the film and

the bonding interactions between atoms. This information can provide insights into the film's chemical properties, such as its composition, purity, and crystallinity. Some specific applications of FTIR spectroscopy in your experiment could include[71].

Identifying the functional groups present in the UHMWPEO polymer, such as the C-O and C-H groups. Analyzing the bonding interactions between the polymer and the metal nanoparticles, such as the coordination of the oxygen atoms with the metal ions. Investigating the presence and bonding of the with SiO_2 nanoparticles in the film. Specifications FTIR (vertex 70) instrument made by Bruker.

3.3.2 Energy Dispersive X-Ray Spectroscopy(EDX)

This technique has been used to study the elements, EDX is a non-destructive technique that can be used to show the purity of materials by multiplying and analyzing them. It can be used for a variety of purposes in engineering, geology, and materials science to analyze the elemental composition of a sample at great spatial resolution. The accuracy of the EDX is however affected by a variety of factors, including the caliber of the SEM instrument, the method of sample preparation, and the calibration of the EDX detector [72].

By using a detector situated close to the sample, EDX measures the energy of the emitted X-rays. Each element has its own set of electron energy levels, and as an electron changes from one level to another, it emits an X-ray with a characteristic energy that is unique to that element. The elements contained in the sample and their relative abundances can be identified by EDX by measuring the energy of the emitted X-ray. Specifications EDX produced by Oxford.

3.3.3 Field Emission Scanning Electron Microscopy (FESEM)

Field Emission Scanning Electron Microscopy is a type of high-resolution microscope that uses the principle of electrons to create high-resolution, three-dimensional content images of the resulting films surfaces. In contrast to a conventional scanning electron microscopy (SEM), which typically uses a thermionic electron source, an FESEM uses a field emission source to produce a much finer electron beam[73].

The FESEM works by applying a high voltage to a small metal tip, causing electrons to be emitted from the tip by a process known as field emission. These accelerating electrons approach the sample, which interact with the surface layer and create an image. The FESEM can obtain much greater resolution and provide more detailed images of the sample surface because the electron beam is much narrower and more defined than conventional SEM, FESEM can be used for a variety of additional analytical approaches in addition to imaging, such as energy dispersive X-ray spectroscopy (EDX) and electron diffraction, FESEM is commonly used in nanotechnology, materials science, and other sectors where high-resolution surface imaging and analysis is critical [74].

Specifications FESEM (Mera-3) system made by T-scan Co., within (1.2 nm at 30 KV) and (2.3 nm at 3 KV), Place, XRD Laboratory – University of Kashan.

3.3.4 X-Ray Diffraction (XRD)

Through X-ray diffraction (XRD) perusing technique it can analyze the crystal structure of the material. This is done by shining X-rays on a sample and measuring the diffraction pattern of the scattered X-rays. The pattern generated by X-rays reveals information about the arrangement of atoms in the material, including the type and size of the crystal lattice, the orientation of the crystals, and

the presence of impurities or defects [75]. This technique was used for the purpose of knowing the crystal arrangement as well as the crystal size was calculated before and after the addition of silica nanoparticles as it can generate generation about its composition, crystal structure, and properties. And XRD can be used to identify unknown materials, study phase transitions and structural changes in materials under different conditions, and to improve material properties for specific applications. It is a non-destructive technique that is widely used in research and industry to develop new materials and analyze existing ones [76]. Specifications XRD (X-pert) produced by Phillips Co., (Nikon-73,346) spectrometer manufactured by Olympus, Place, XRD Laboratory – University of Kashan.

3.3.5 Ultraviolet-Visible Spectrophotometer (UV- VIS)

In order to measure the absorption and transmission of light in the ultraviolet visible part of the electromagnetic spectrum, a UV-VIS spectrophotometer is a frequently used device in materials research. We can examine the electrical and structural characteristics of materials, including membranes and nanoparticles, using this non-destructive method. A UV-VIS spectrophotometer can be used to measure the optical characteristics of the UHMWPEO/Cu NPs/Ag-SiO_2 films created in our experiment. We may learn about the film thickness, refractive index, extinction coefficient, and bandgap energy by measuring the absorption or transmission of light at various wavelengths. These variables, such as the film's transparency, color, and capacity to absorb or reflect light, might shed light on how the film behaves optically [77]. Specifications UV/visible properties were studied by a double beam Shimadzu (1800) spetrometer.

4.1 Introduction

This chapter contains the results and discussion of the structural and optical properties of the (UHMWPEO/Cu NPs/Ag NPs) blend before and after adding different weights from silica nanoparticles (SiO_2) that prepared by casting method at room temperature (30±5)°C. Structural and optical properties, such as, FTIR, EDX, FESEM, XRD and UV-VIS have also been investigated. .

4.2 Structural Properties

In this paragraph several measurements are included

4.2.1 Fourier Transform Infrared Rays (FTIR)

Fourier Transform Infrared Rays spectroscopy is an important technique for the investigation of composite structure, as it provides information about the complication and interactions between the various constituents in this composite complexes. Fourier transforms infrared spectroscopy analysis of (UHMWPEO/Cu/Ag) nanocomposite at room temperature in the frequency region of (450–4000) cm^{-1}. The main function of using FTIR is to evaluate the type of chemical bonding between different phases that are present, examine if there is a chemical reaction occurs or it is merely physical blending and qualitatively analyze the materials, which are in the bulk of films.

All spectra exhibit the characteristic absorption bands of (UHMWPEO/Cu/Ag) composite, the new bonds formed in this cover will be explained according to the following figures and bond tables[78].

Figure (4.1) and table (4.1) represent the FTIR spectrum of (UHMWPEO/ Cu/Ag) nanocomposite. In this Figure we show that in appeared in (3959, 3829, 3445, 2870, 2512, 2355, 2235, 2165, 2097, 1965, 1801, 1638, 1460, 1350, 1280, 1099, 846, 579and 528)cm^{-1} related to (N-H,N-H,O-H,C-H, C≡N, C≡N, C≡C, C≡C, C≡C, C=O, C=C, C=C, C-N, C-N, C-O, C-O, C-C, C-C and C-C) Where the peaks of the polymer appeared between the wavenumber from (2000-2500) cm^{-1} and the results are identical to the study[41].

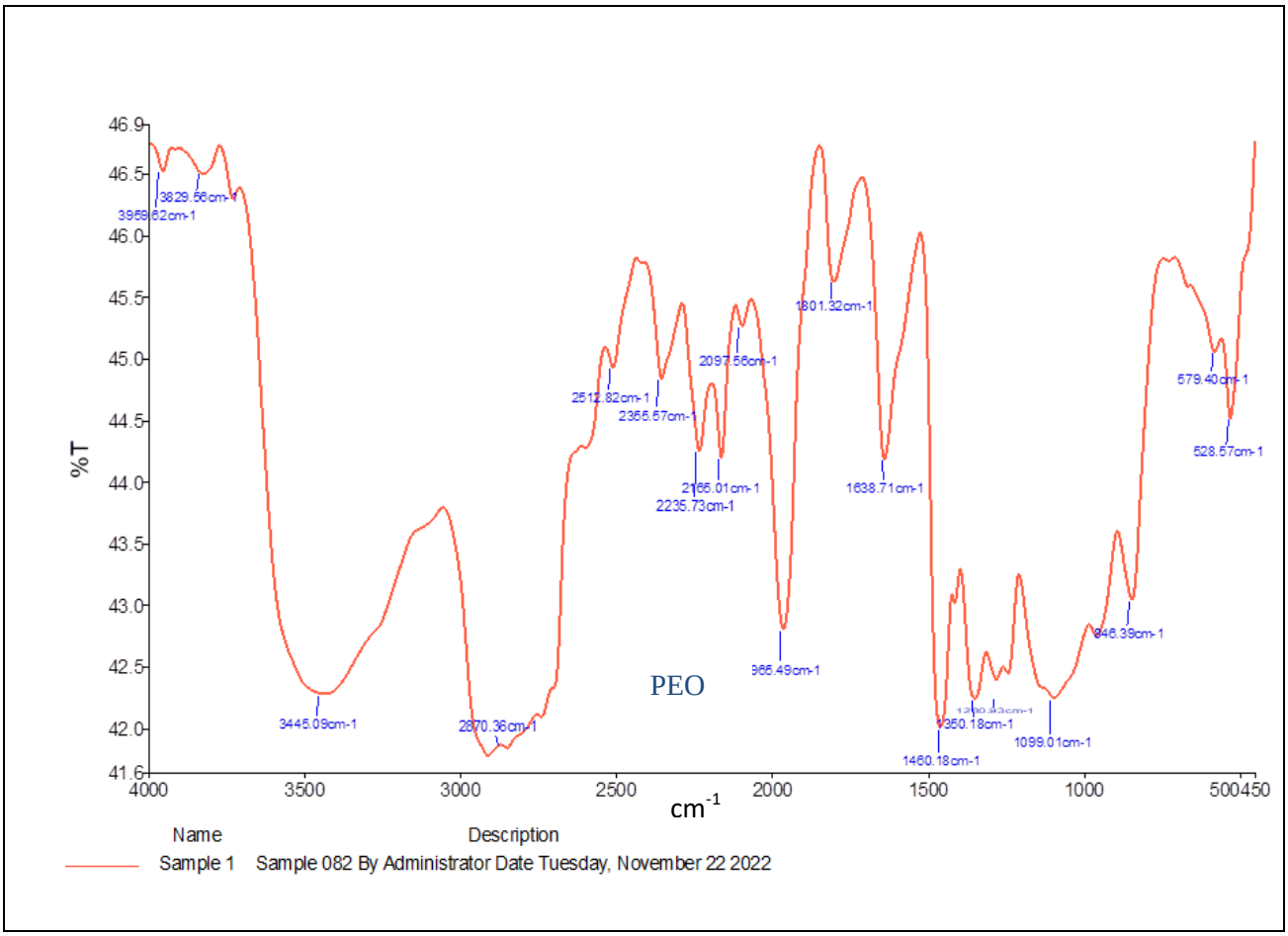

Fig. (4.1): FTIR Spectrum of (UHMWPEO/Cu/Ag) Nanocomposite.

Table (4.1): FTIR Transmittance Bands Positions and Their Assignments for the (UHMWPEO/Cu/Ag) Nanocomposites.

Composite	Wavenumber cm^{-1}	Type of Bond
(UHMWPEO/ Cu/Ag) Nanocomposite	3959.62	N-H
	3829.56	N-H
	3445.09	O-H
	2870.36	C-H
	2512.82	C≡N
	2355.57	C≡N
	2235.73	C≡C
	2165.01	C≡C
	2097.56	C≡C
	1965.49	C=O
	1801.32	C=C
	1638.71	C=C
	1460.18	C-N
	1350.18	C-N
	1280.93	C-O
	1099.01	C-O
	846.39	C-C
	579.40	C-C

For the experimental data presented in the following Figures, after adding silica nanoparticles in different proportions (0.05,0.07 and 0.09 from SiO_2) the formation of some new chains was observed as shown in Figures (4.2), (4.3) and(4.4) for each addition ratio.

We observed through (FTIR) if SiO_2 nanoparticles are present in (UHMWPEO/ Cu/Ag) Nano composites it leads to molecular vibrational motion restriction, especially vibrational motion in three dimensions of the superposition because new levels are being formed within matter, and will most likely be affected by IR energy. Therefore, the nano composites have the property of nonporous which is almost limiting [79].

The Fourier analysis infrared spectroscopy (FTIR) spectra of nano films and doped nano films correspond to silica nanoparticles [80].No new peaks were appeared after loading the SiO_2 , but there is small peaks shift less than 10 cm^{-1} as shown in tables (4.2),(4.3) and(4.4).

These results confirm that there is no any chemical interaction happens between the matrix material and the loading material, the physical interaction , was happened as appear from the increasing of the nitrates of peaks of the incorporation[81,82].

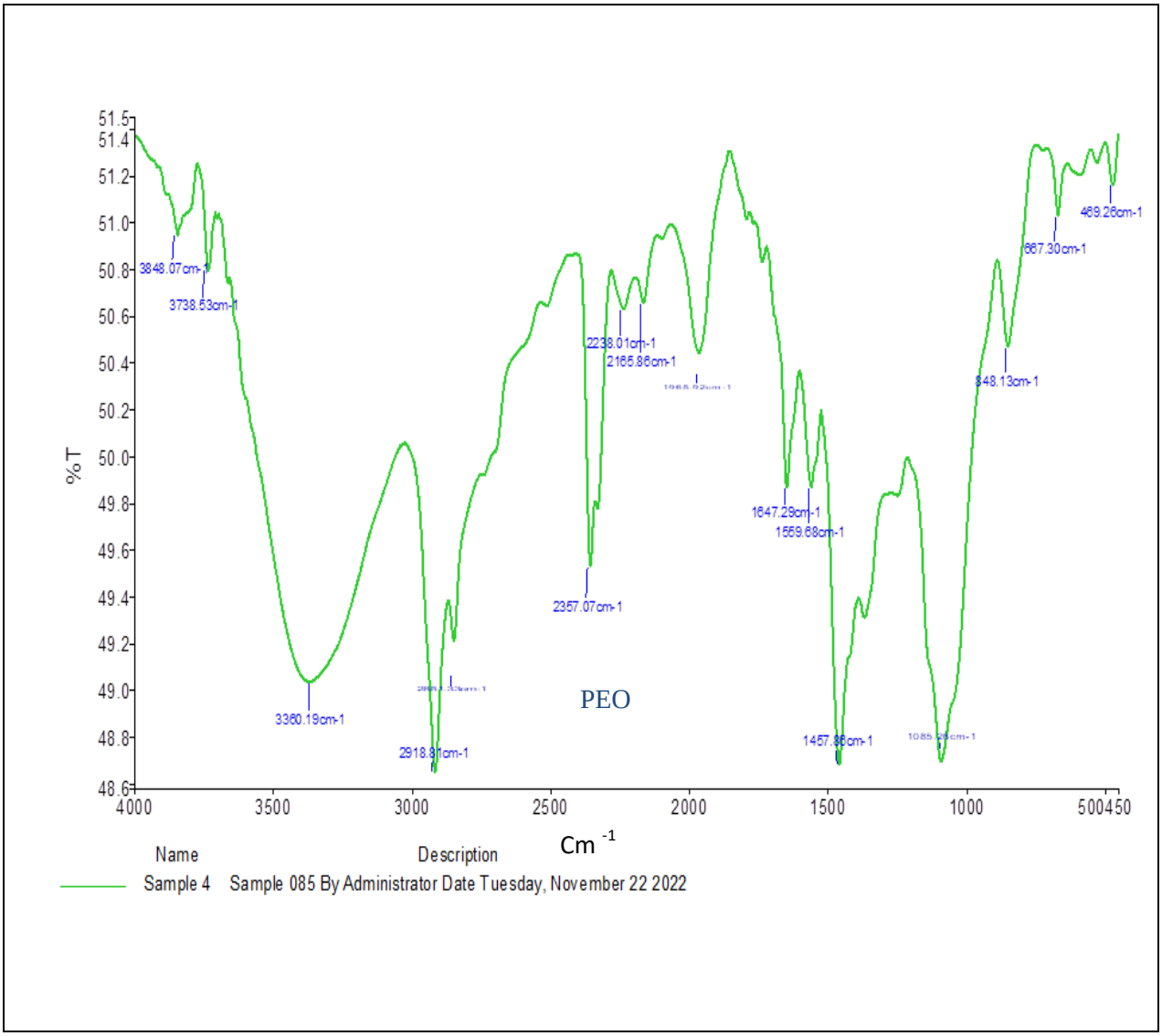

Fig. (4.2): FTIR Spectrum of (UHMWPEO/Cu/Ag) Nanocomposite with (0.05 SiO_2).

Been noticedfrom Figures (4.1) to (4.4) that there is same bonds were hidden after incorporation of SiO_2 and this is way be correlated with the effect of strong interaction (physical interaction) which happed between the host (UHMWPEO/ CuNPs/ AgNPs) and silica NPs.

Table (4.2): FTIR Transmittance Bands Positions and Their Assignments for the (UHMWPEO/Cu/Ag) Nanocomposite, with (0.05 SiO_2).

Composite	Wavenumber cm^{-1}	Type of Bond
UHMWPEO/Cu /Ag Nanocomposite + (0.05) SiO_2	3848.07	N-H
	3738.53	N-H
	3360.19	O-H
	2918.81	C-H
	2851.33	C-H
	2357.07	C≡N
	2238.01	C≡C
	2165.86	C≡C
	1965.92	C≡C
	1647.29	C=C
	1559.68	C=C
	1457.86	C-N
	1085.26	C-O
	848.13	C-C
	667.30	C-C
	469.26	C-C

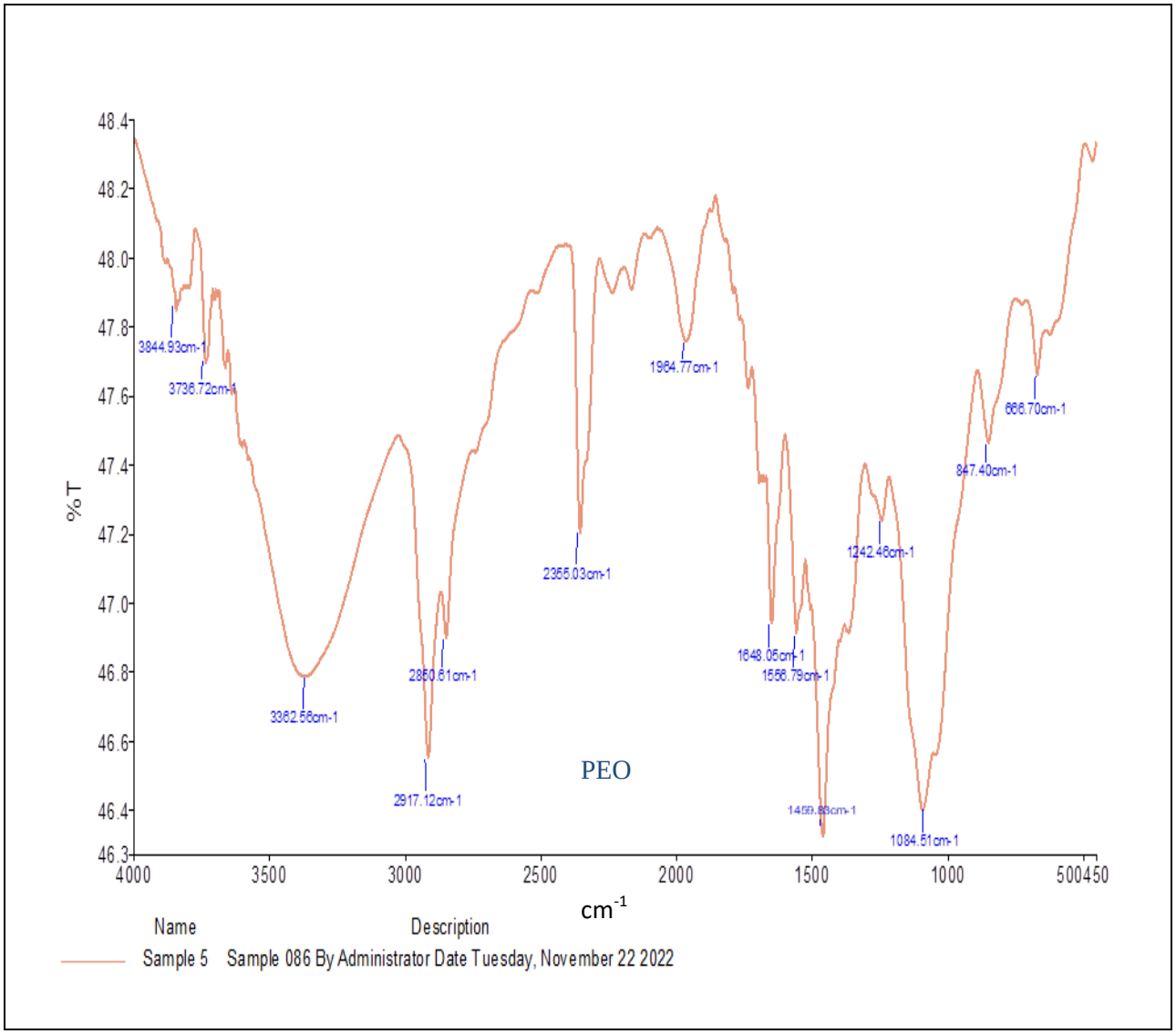

Fig. (4.3): FTIR Spectrum of (UHMWPEO/Cu/Ag) Nanocomposite with(0.07SiO_2).

Table (4.3): FTIR Transmittance Bands Positions and Their Assignments for the (UHMWPEO/Cu/Ag) Nanocomposite, with (0.07 SiO_2).

Composite	Wavenumber cm^{-1}	Type of Bond
UHMWPEO/Cu/Ag Nanocomposite + (0.07) SiO_2	3844.93	N-H
	3736.72	N-H
	3362.56	O-H
	2917.12	C-H
	2850.61	C-H
	2355.03	C≡N
	1964.77	C≡C
	1648.05	C=C
	1556.79	C=C
	1459.83	C-N
	1242.46	C-0
	1084.51	C-O
	847.40	C-C
	666.70	C-C

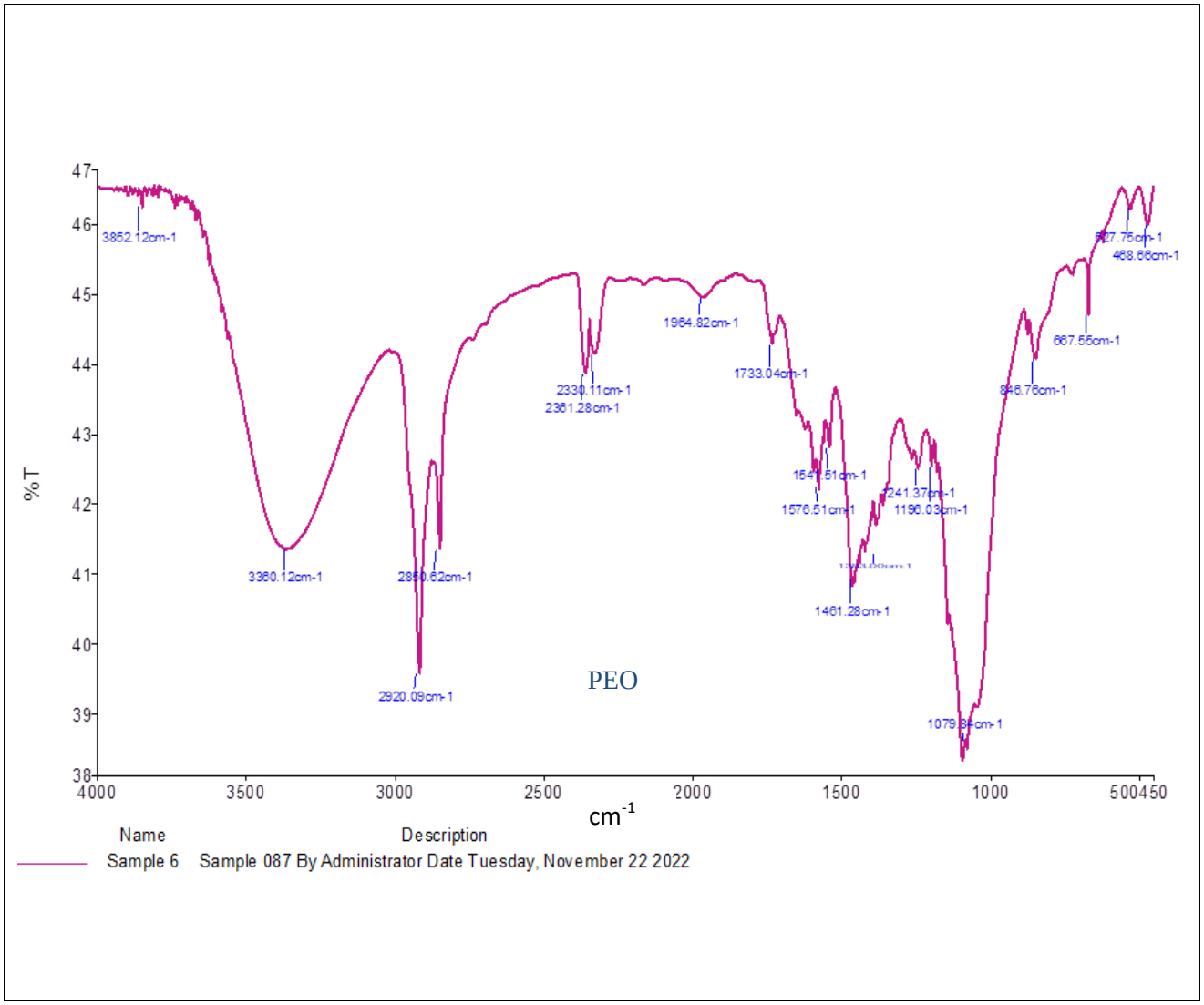

Fig. (4.4): FTIR Spectrum of (UHMWPEO/Cu/Ag) Nanocomposite with (0.09 SiO_2).

Table (4.4): FTIR Transmittance Bands Positions and Their Assignments for the (UHMWPEO/Cu/Ag) Nanocomposite, with (0.09 SiO_2).

Composite	Wavenumber cm^{-1}	Type of Bond
UHMWPEO/Cu/Ag Nanocomposite + (0.09) SiO_2	3852.12	N-H
	3360.12	O-H
	2920.09	C-H
	2850.62	C-H
	2361.28	C≡N
	2330.11	C≡N
	1964.82	C≡C
	1733.04	C=O
	1576.51	C=C
	1541.51	C=C
	1461.28	C-N
	1383.00	C-N
	1241.37	C-O
	1079.84	C-O
	846.76	C-C

4.2.2 Energy Dispersive X-ray Spectroscopy (EDX)

An analytical technique used to analyze elements to determine the chemical properties of samples, and it is a type of X-ray spectroscopy.In this technique, both oxygen and carbon appeared to represent the polymer, as well as the appearance of copper and silver only, and this represents the superimposed as a base[83]. Figure (4.5) the atomic and weight ratios of the components of the composite free of silica nanoparticles are indicated.

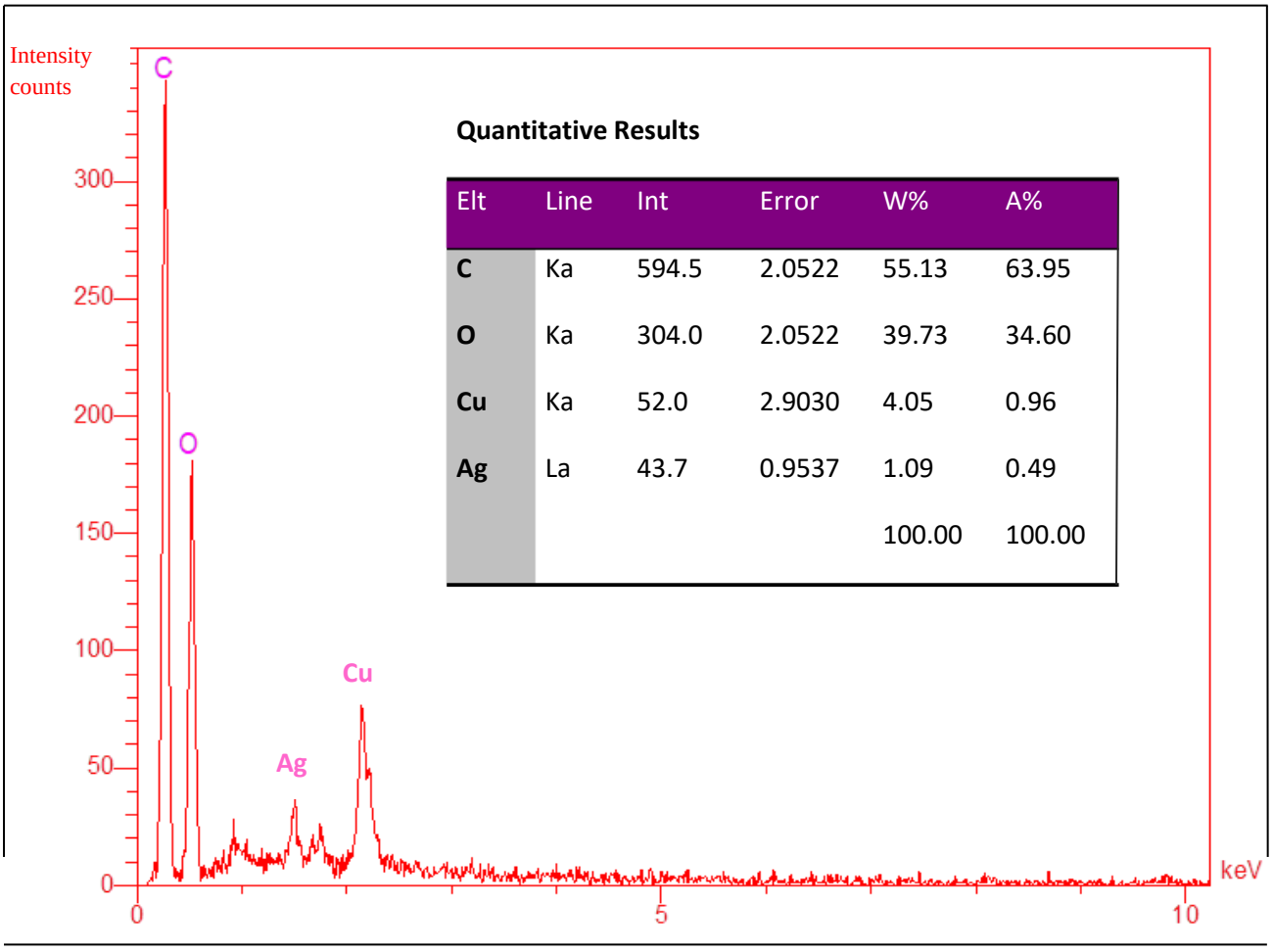

Quantitative Results

Elt	Line	Int	Error	W%	A%
C	Ka	594.5	2.0522	55.13	63.95
O	Ka	304.0	2.0522	39.73	34.60
Cu	Ka	52.0	2.9030	4.05	0.96
Ag	La	43.7	0.9537	1.09	0.49
				100.00	100.00

Fig. (4.5): EDX of (UHMWPEO/Cu/Ag) Nanocomposite.

Figure (4.6) shows the spread of silica nanoparticles in the overlay, where the silica nanoparticles appeared in this technique as part of the components of that overlay[84].

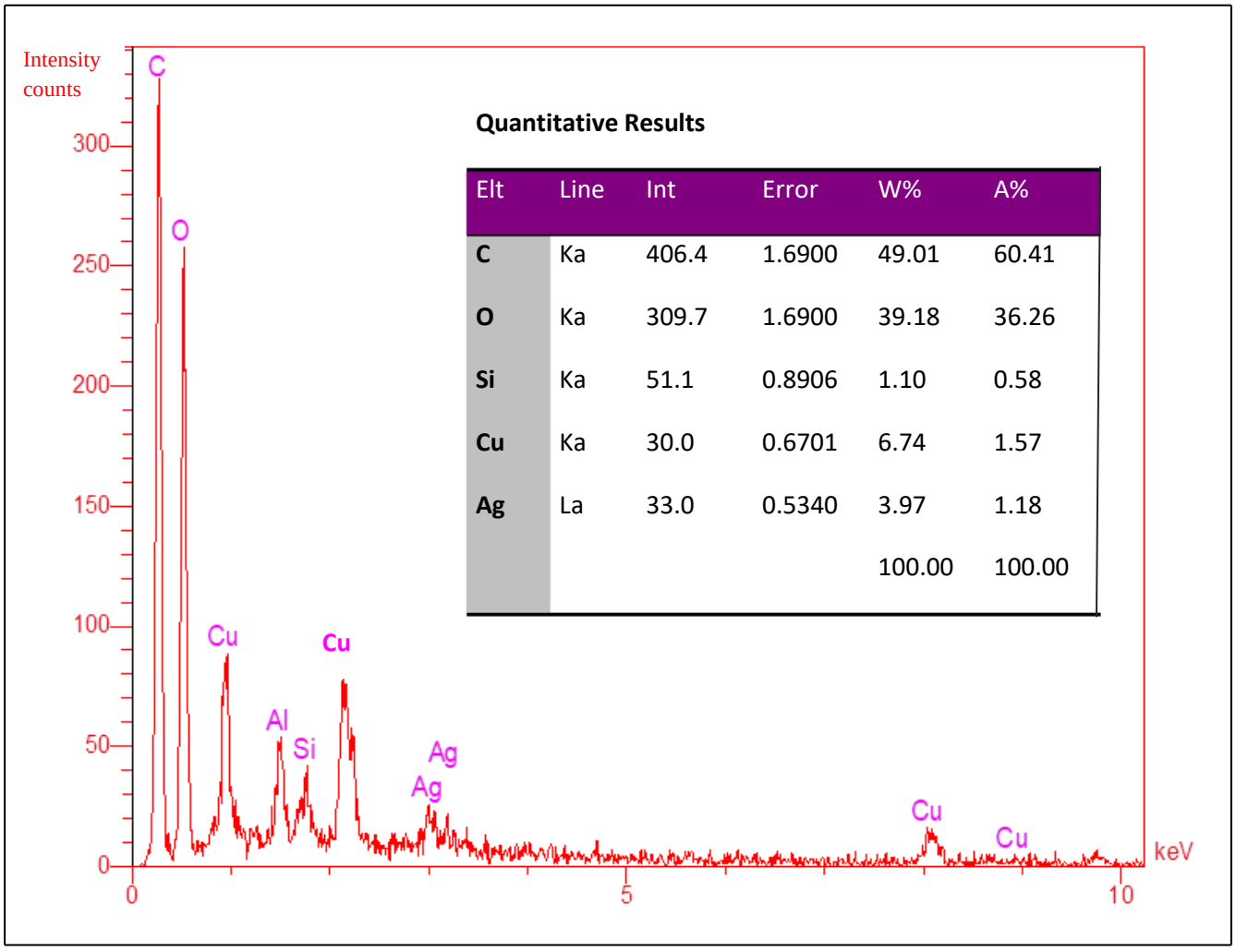

Fig. (4.6): EXD of (UHMWPEO/Cu/Ag) Nanocomposite with (SiO_2).

4.2.3 Field Emission Scanning Electron Microscopy (FESEM)

The results FESEM was used to fully investigate the effect of nanoparticle content and to examine the particle dispersion in the composite matrix and the interaction or agglomeration of the nanoparticles. Figure (4.7) shows typical FESEM images of pure silica particle-free UHMWPEO/Cu/Ag films where the polymers are softer, more homogeneous and cohesive. It is clear from the current figure that there was no aggregation or cracking in the resulting films between these input materials. Where spherical shapes appeared as a result of copper nanoparticles and silver nanoparticles, which led to basic formations such as bimetallic nanoparticles. The Cu/Ag additions were fine and homogeneously distributed within the UHMWPEO matrix and this is probably due to the ability of this polymer to integrate with the particles of the nanocomposite[85,86]. The results of the images showed that the grain size 35.7nm.

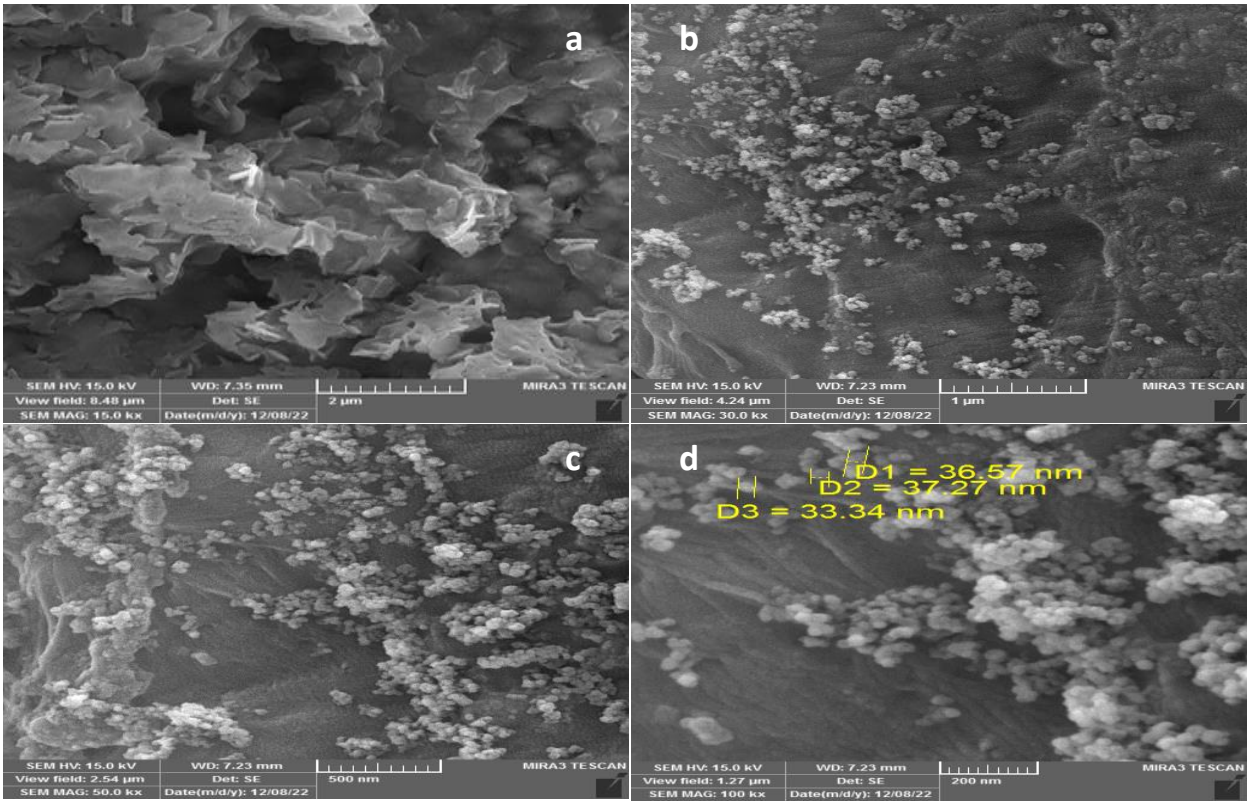

Fig. (4.7): FESEM Images of (UHMWPEO/Cu/Ag) Nanocomposite. (a):15 kx, (b): 30kx, (c): 50 kx, (d): 100 kx.

Figure (4.8) below shows typical images of nanocomposite (UHMWPEO/ Cu/ Ag-SiO_2) films with (0.05) wt% from silica within the composite content. The addition of nanoparticles to the superposition is evident in the surface morphology of this system. It is evident from the images that the grains accumulate an increasing proportion of nanoparticles. The conformational shape of the nano composite (UHMWPEO/ Cu/Ag-SiO_2) films was formed from aggregates or cut randomly on the top surface. The results shows an increase in the number of white spheres on the surface with nanoparticles particles concentration more the films display a uniform density of grain distribution in the surface morphology. The results indicate that the nanoparticles tend to form well-dispersed agglomerates in the composite films, with an grain size of 35.8 nm. It is understood that the nanoparticles (SiO_2) are randomly distributed in (UHMWPEO / Cu / Ag) membranes. It was concluded that small agglomerates are formed, making the membranes softer [87].

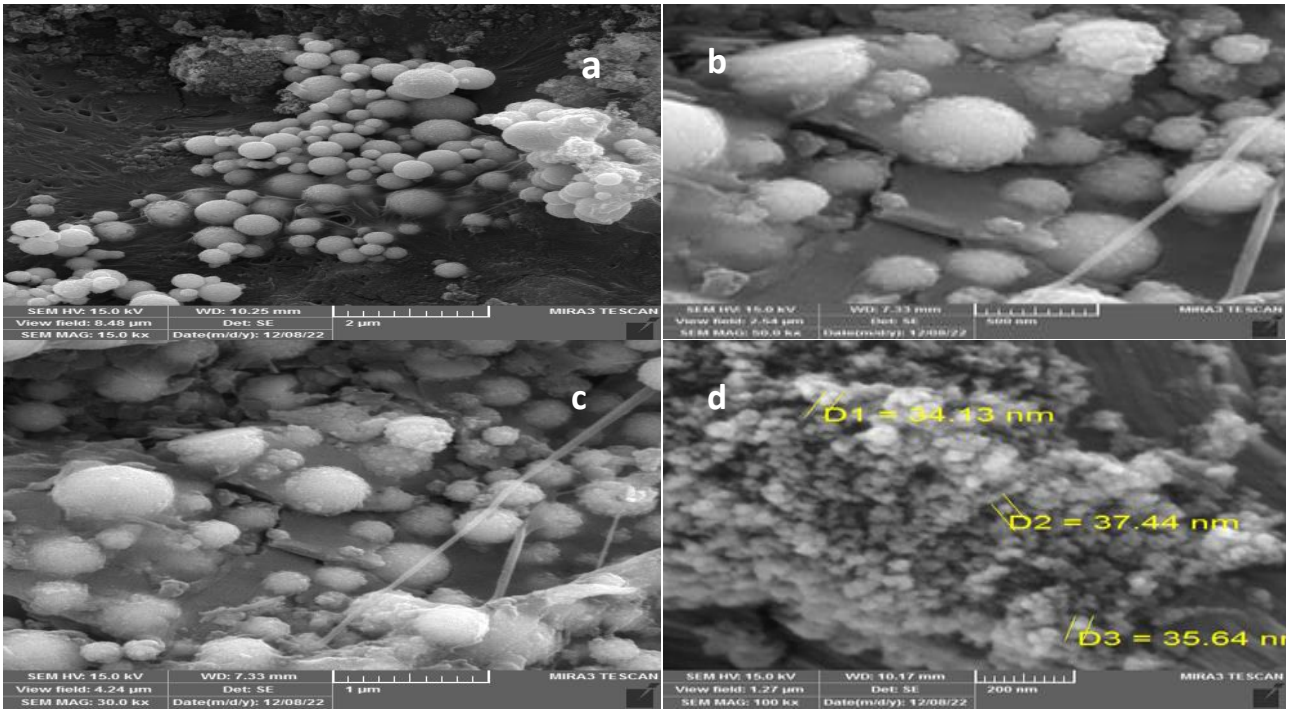

Fig. (4.8): FESEM Images of (UHMWPEO/Cu/Ag) Nanocomposite with (0.05 SiO_2) (a):15 kx, (b): 30 kx, (c): 50 kx, (d): 100 kx.

Figures (4.9) and (4.10) show images of the compound (0.07 and 0.09) wt.% by increasing the amount of SiO_2 in (UHMWPEO/Cu/Ag) films, greatly enhancing the distribution, and nanoparticles are formed. A continuous network inside the polymer, and it appeared in different and distinct shapes, such as spherical and flowery, with clear growth of grain size (45.8)nm. This network includes channels in which charge carriers are allowed to pass through, changing the material properties [88]. This is in line with the researchers' findings [89].

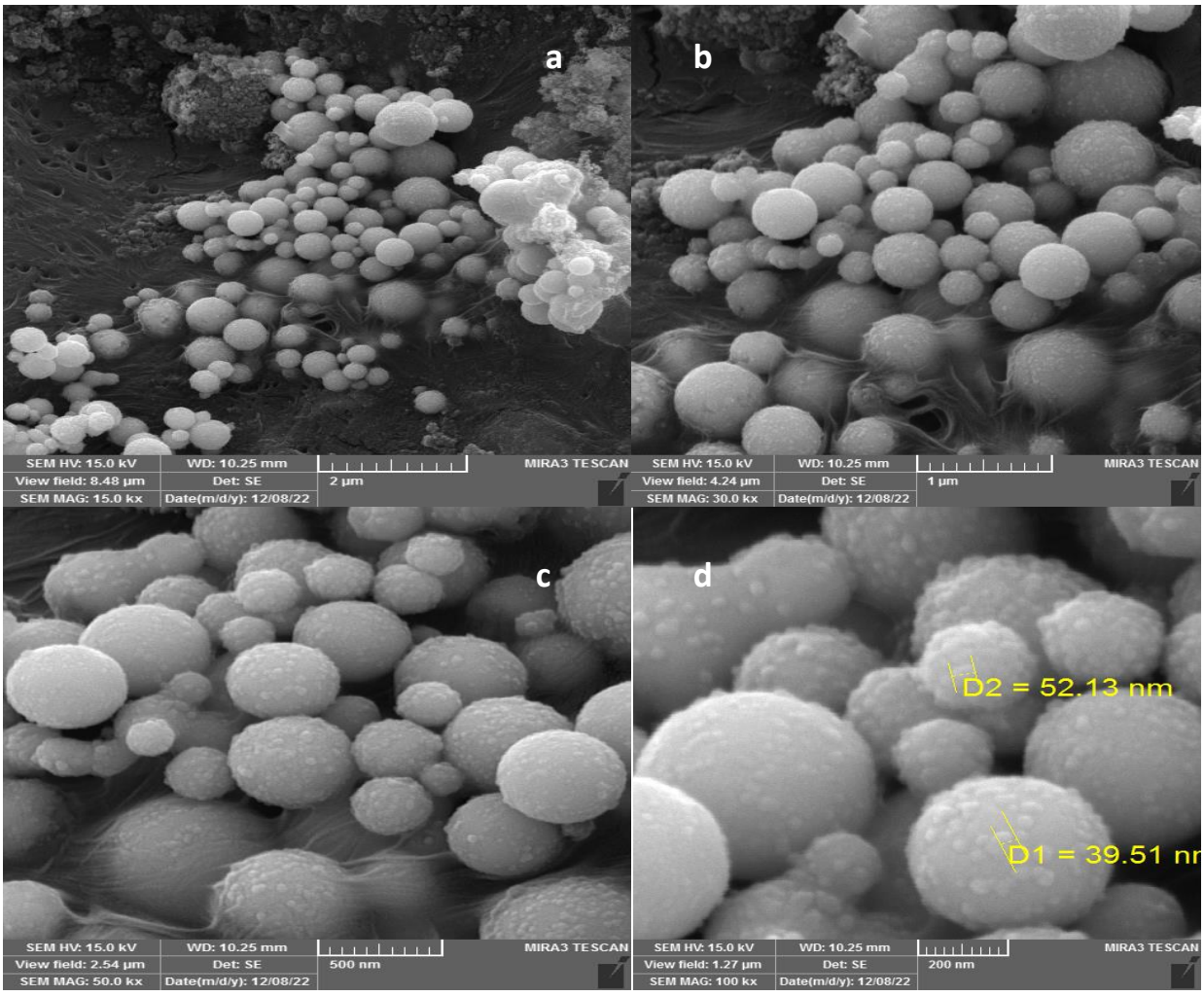

Fig. (4.9): FESEM Images of (UHMWPEO/Cu/Ag) Nanocomposite with (0.07 SiO_2) , (a):15 kx, (b): 30 kx, (c): 50 KXkx, (d): 100 kx.

By increasing the amount of SiO_2 in the (UHMWPEO/Cu/Ag) films, the distribution is greatly improved, and the nanoparticles create a flower-shaped network within the polymer with a grain size of up to(54.2)nm . This network includes channels in which charge carriers are allowed to pass through, changing the properties of materials. This is in line with the findings of the researchers [90].

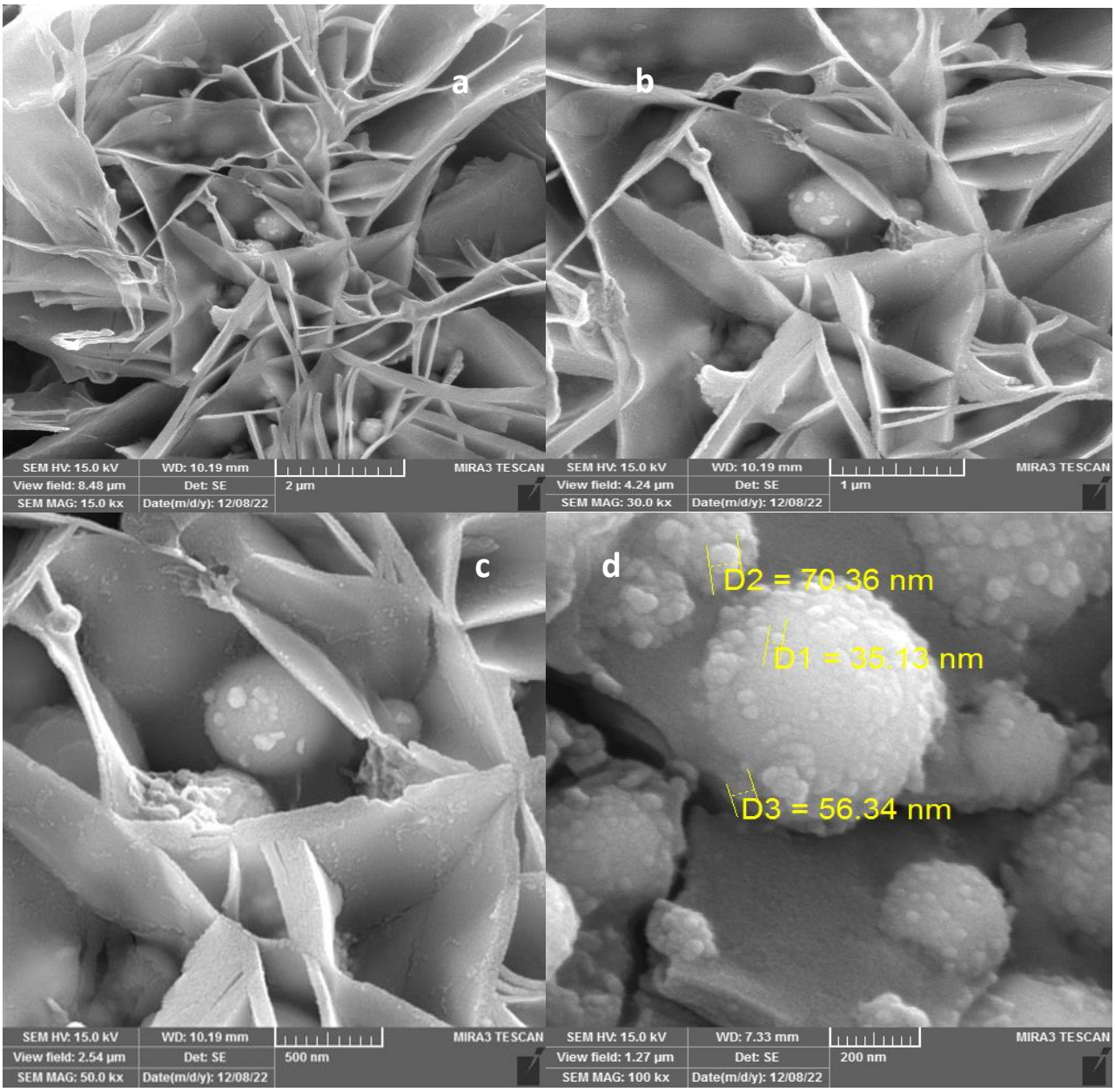

Fig. (4.10): FESEM Images of (UHMWPEO/Cu/Ag) Nanocomposite with (0.09 SiO_2) , (a):15 kx, (b): 30 kx, (c): 50kx, (d): 100 kx.

4.2.4 X-ray Diffraction (XRD)

Through a technique (XRD) we can know the crystal structure of the resulting films (UHMWPEO / Cu NPs / Ag NPs) and the nature of their growth, where the study was carried out in multiple stages before and after adding silica (SiO_2) to the matrix.

The X-ray diffraction patterns of the (UHMWPEO/ Cu NPs/Ag NPs) superimposed film is shown in Figure (4.11) and table (4.5) and it was found that the film of the superimposed has a semicrystalline nature and grows in a rhombohadral crystalline structure.

It was observed that the main peaks appeared at $2\Theta = 18.5°$ and 24.04° corelateed to UHMWPEO polymer with miller indices (110) and (021) respectively. The observed diffraction patterns are in good agreement with the standard PEO with code number (JCPDS 49-2200) [91].

The peaks apeared at $2\Theta = 38.07°$ agreed with (Ag) with miller indices (111), and the observed diffraction patterns are in good agreement with the standard PEO with code number (JCPDS 04-0782)[92].

The other peaks at $2\Theta = 43.22°$ and 50.33° with miller indices (100), (200) represent (Cu) and the observed diffraction patterns are in good agreement with the standard PEO with code number (JCPDS 70-3083)[93].

Due to the amorphous stretcher of silica and the small amount of it in this composite, therefore the silica does not show any peaked structure. The results showed that the composite is semicrystalline in nature and grows into a rhombohadral crystallinity[94].

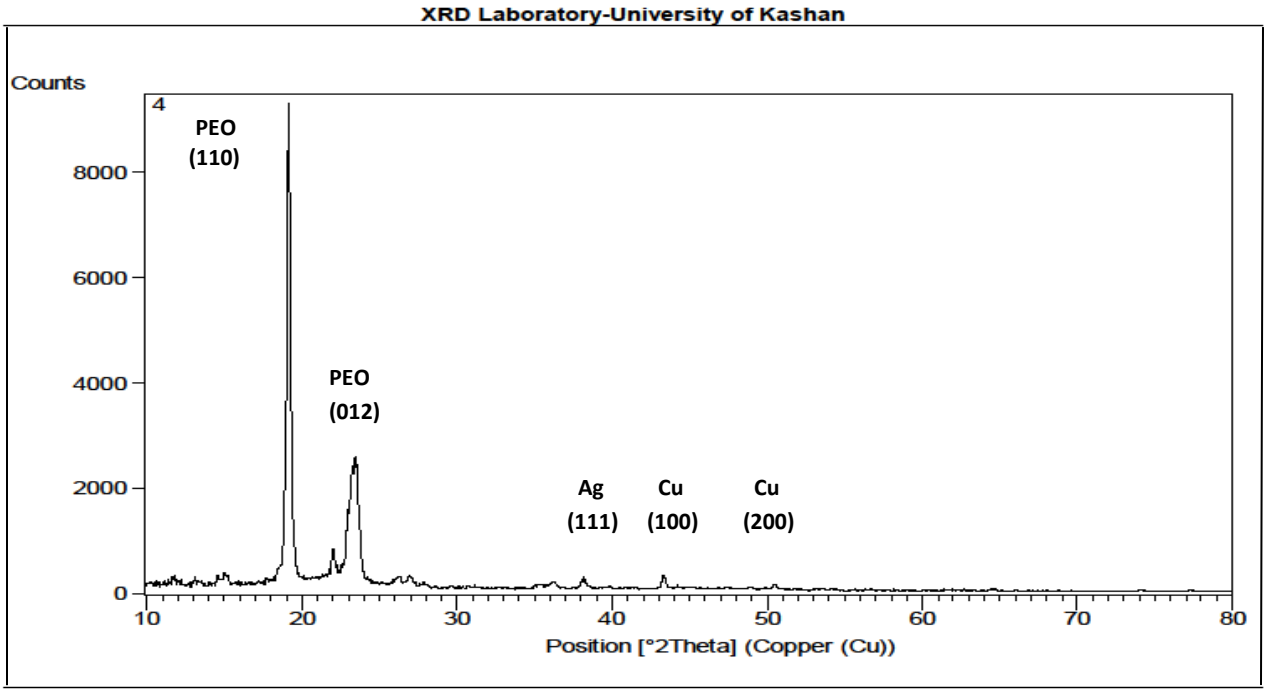

Fig. (4.11):X- Ray Diffraction Pattern of (UHMWPEO/Cu NPs/Ag NPs) Nanocomposite.

Table (4.5): Obtained Results from the XRD for (UHMWPEO/Cu NPs/Ag NPs) Nanocomposite.

Sample	**2Θ degree**	***(hkl)***	**FWHM (degree)**	**Crystal Size nm**
PEO	18.50	110	0.389	26.0
PEO	24.04	012	0.352	29.9
Ag	38.07	111	0.393	21.3
Cu	43.22	100	0.196	43.4
Cu	50.33	200	0.295	29.7
				Av=30.06

Figure (4.12) and table (4.6) show the X-ray diffraction pattern of the (UHMWPEO/Cu NPs/Ag NPs) Nanocomposite film doped in 0.05 wt.% silica (SiO_2). It was observed that the main peaks appeared at 2Θ = 18.23° and 24.05° corelateed to UHMWPEO polymer with miller indices,(021) and (012). And the other peaks represent (Ag) by 2Θ = 36.13° with miller indices (111). The (Cu) by 2Θ = 43.43° and 50.49° with miller indices (111), (200) respectively, and this is identical to (JCPDS Card No. 01 - 086 - 1561) for Ag NPs @ Cu NPs.

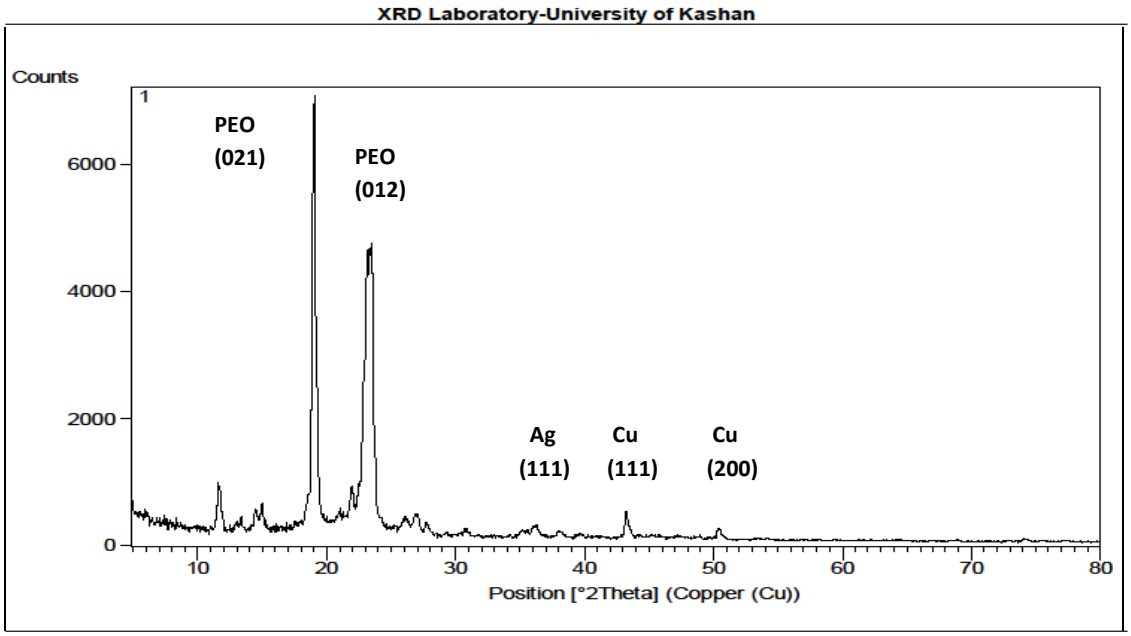

Fig. (4.12):X- Ray Diffraction Pattern of (UHMWPEO/Cu NPs/Ag NPs) Nanocomposite with (0.05 SiO_2) .

Table (4.6): Obtained Results from the XRD for (UHMWPEO/Cu NPs/Ag NPs) Nanocomposite with (0.05 SiO_2) .

Sample	2Θ degree	*(hkl)*	FWHM (degree)	Crystal Size nm
PEO	18.23	021	0.237	35.1
PEO	24.05	012	0.152	56.4
Ag	36.13	111	0.295	28.3
Cu	43.42	111	0.225	43.4
Cu	50.49	200	0.360	22.4
				Av=37.12

Figure(4.13) and table (4.7) show the X-ray diffraction pattern of (UHMWPEO/Cu NPs/Ag NPs) composite film doped in (0.07) wt.% silica (SiO_2), mainly appeared for polymer 2Θ 18.20ºand 2Θ = 24.04º, with miller indices (021) and (012) respectively. And other peaks represent (Ag) 2Θ = 36.21º with miller indices(111), and (Cu) 2Θ = 43.03ºand 2Θ = 50.36º with miller indices(111),(112). . This may be due to the improvement and increase in granular size. The increase in grain size of the film (UHMWPEO/Cu NPs/Ag NPs/SiO_2). The results show that the superposition is semicrystalline in nature and grows into a rhombohadral crystal.[95,96]

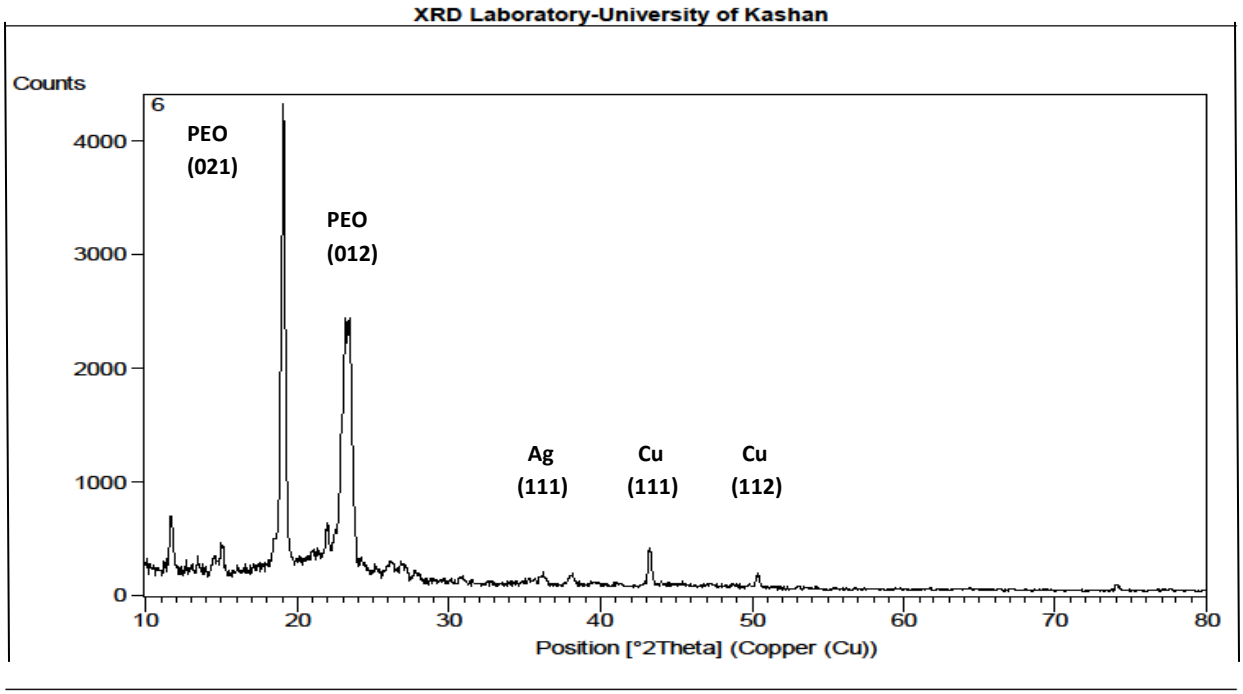

Fig. (4.13):X- Ray Diffraction Pattern of (UHMWPEO/Cu NPs/Ag NPs) Nanocomposite with (0.07 SiO_2) .

Table (4.7): Obtained Results from the XRD for (UHMWPEO/Cu NPs/Ag NPs) Nanocomposite with (0.07SiO_2) .

Sample	2Θ degree	*(hkl)*	FWHM (degree)	Crystal Size nm
PEO	18.20	021	0.246	33.8
PEO	24.04	012	0.243	34.6
Ag	36.21	111	0.393	21.2
Cu	43.03	111	0.197	45.2
Cu	50.36	112	0.246	22.9
				Av=31.54

The crystal linty size was increased after loading this means that the silica effectively grows in the matrix. There is no any new peak append after adding the silica due the fact that small amounts of it was incorporated to the matrix but some matrix peaks were effected after adding and same peaks and decrease other hidden and broaded.

Figure(4.14) and Table (4.8) show the X-ray diffraction pattern of the (UHMWPEO/ Cu NPs /Ag NPs) composite film doped in (0.09) wt.% silica (SiO_2), mainly appeared for polymer $2\Theta = 18.56^{o}$and $2\Theta = 21.34^{o}$, with miller indices (021) and (300) respectively.

The other peaks represent (Ag) $2\Theta = 38.13^{o}$ with miller indices(111) and (Cu) $2\Theta = 43.03^{o}$and $2\Theta = 50.44^{o}$ with miller indices(111),(110) , The increase in grain size of the film (UHMWPEO/Cu NPs/Ag NPs/SiO_2) indicates that the result is approximately close to [97].

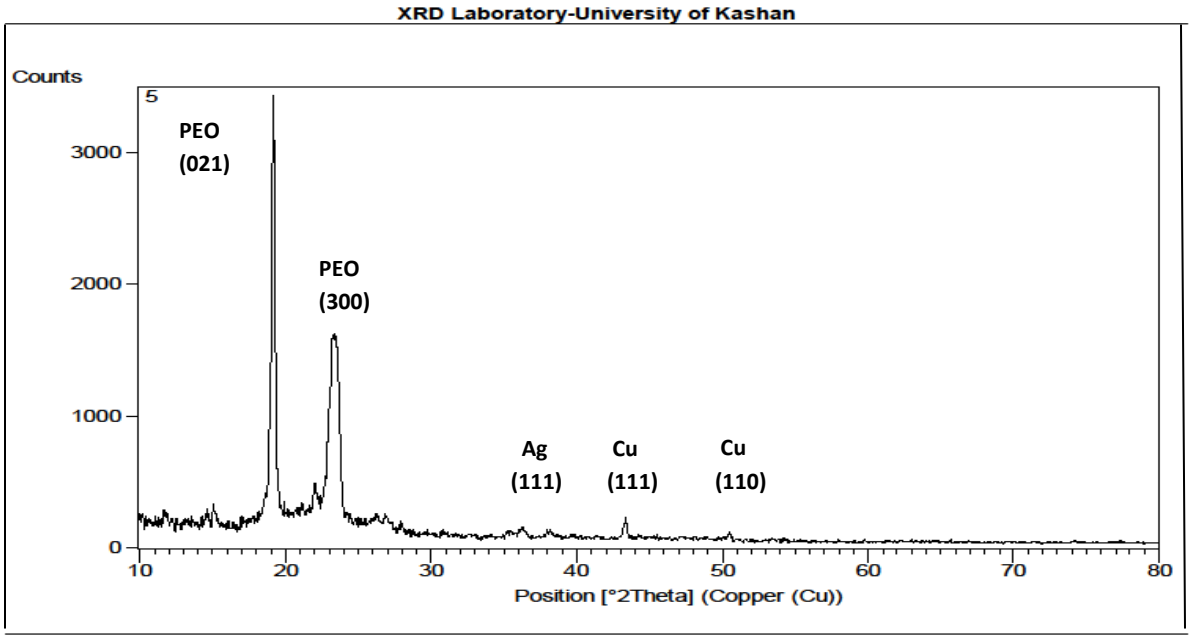

Fig. (4.14):X- Ray Diffraction Pattern of (UHMWPEO/Cu NPs/Ag NPs) Nanocomposite with (0.09 SiO_2) .

Table (4.8): Obtained Results from the XRD for (UHMWPEO/Cu NPs/Ag NPs) Nanocomposite with (0.09 SiO_2) .

Sample	2Θ degree	*(hkl)*	FWHM (degree)	Crystal Size nm
PEO	18.56	021	0.239	34.8
PEO	21.34	300	0.189	44.7
Ag	38.13	111	0.393	40.4
Cu	43.03	111	0.243	36.3
Cu	50.44	110	0.300	29.2
				Av=33.7

4.3 Optical Properties

The main purpose of studying the optical properties of the (UHMWPEO/Cu/Ag) nanocomposites is to identify the effect of adding the silica (SiO_2) nanoparticles on the optical properties. UV-VIS spectroscopy was used to show the optical properties of this composite .A complete impression has been taken on the important optical properties of this composite.

The research covers the recording of the spectra of absorbance for the (UHMWPEO/Cu/Ag) films at room temperature before and after the addition of silica nanoparticles and calculating the transmittance, absorption coefficient, extinction coefficient and other optical constants ,as well as calculating the energy gaps[98].

4.3.1 Absorbance (A)

Figure (4.15) show the absorption spectra of (UHMWPEO/Cu/Ag) nanocomposites before and after the addition of silica nanoparticles, as a function of the wavelength of the incident light. It can be noticed from the figure that the absorbance for all films have a high values at wavelength in the neighborhood of the fundamental absorption edge (300)nm, then the absorbance decreases with the an increasing of wavelength. In general, the absorbance of the films has low values in the visible and near infrared region. This behavior can be explained as follows, at high wavelength the incident photons doesn't have enough energy to interact with atoms. Thus the photon will be transmitted, when the wavelength decreases, the interaction between incident photon and material will occur, and then the absorbance will increase [99]. In other words absorb the incident light by the free electrons. Consequently, by the increase of the weight percentages of nanoparticles, absorbance is increased, these results are similar to the results reached by the researchers [100]. We notice an increase in the absorbance when adding SiO_2.

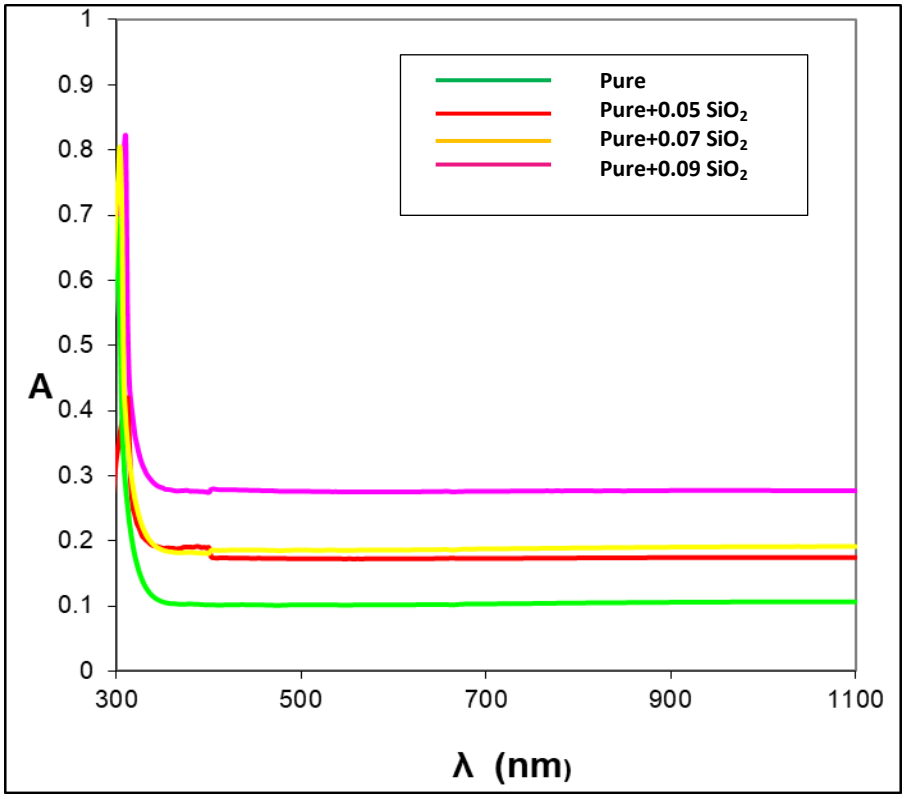

Fig. (4.15): Absorbance Behavior of (UHMWPEO/Cu/Ag-SiO_2).

It has been observed that the films that possess silica nanoparticles have a higher absorption spectrum, and this indicates an increase in the density of the overlay as a result of the diffusion of silica nanoparticles within the overlay [101].

4.3.2 Transmittance (T)

The additional (SiO_2) nanoparticles have electrons in their outer orbits that can take in the incident light's electromagnetic energy and move to higher energy levels by doing so. Because the traveling electron has filled open spots in the energy bands and part of the incident light is absorbed, this process does not result in radiation emission, Figure (4.16) demonstrates that transmittance reduces as nanoparticle concentration rises.

While there are no free electrons in polyethylene oxide (electrons are bound to atoms by covalent bonds), this results in the necessity for a photon with a high energy to break the electron bond and transfer the electron to the conduction band [102].

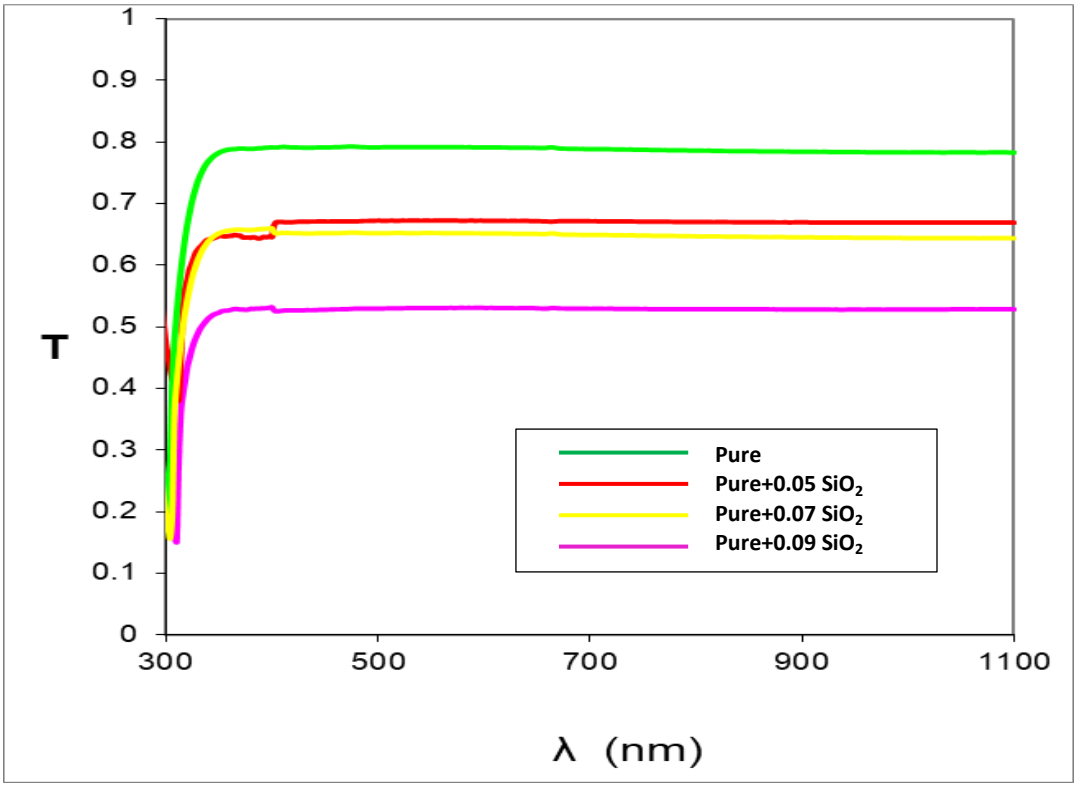

Fig. (4.16): Transmittance Behavior of (UHMWPEO/Cu/Ag-SiO_2).

4.3.3 Reflectivity (R)

Under the energy conservation the reflectance of pure and doped was calculated. The relationship between reflectivity and wavelengths for a pure(UHMWPEO/Cu/Ag) nanocomposite and doped with a varied ratio of SiO_2 is shown in Figure (4.17).

It is clear that for short wavelengths, reflectivity rises as wavelength increases. With increasing wavelength and increasing deflection for long wavelengths,

reflectivity increases for short wavelengths while decreasing for long wavelengths [101,102]. According to the law of conservation of energy in relation exemplified by equation (2.4)

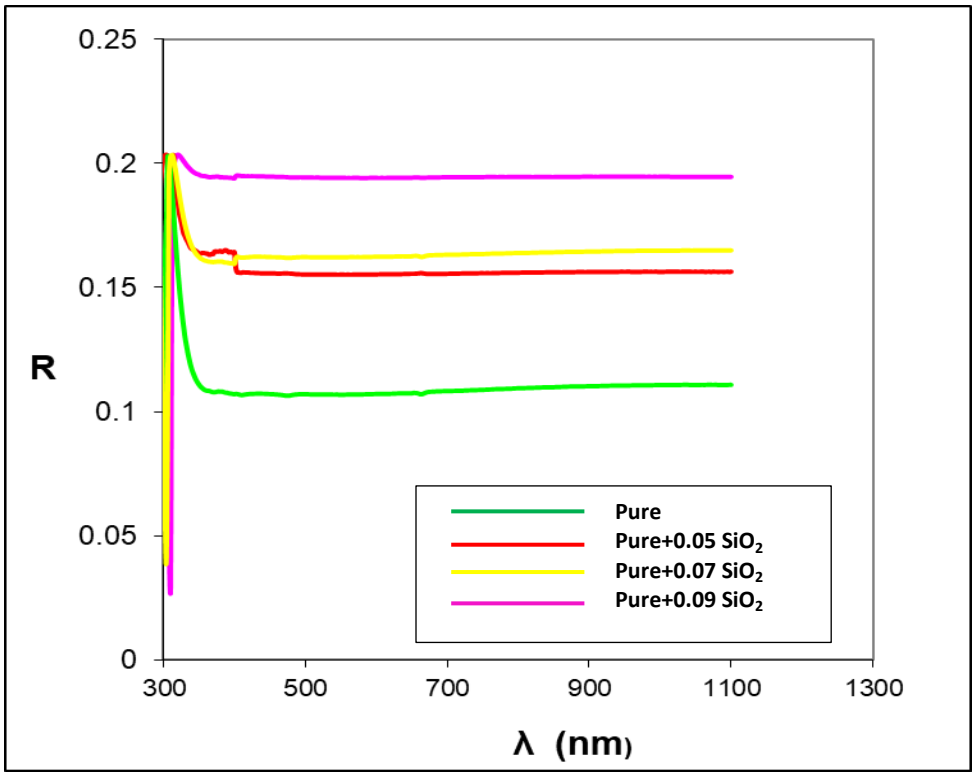

Fig. (4.17): Reflectivity Behavior of (UHMWPEO/Cu/Ag-SiO_2).

4.3.4 The Absorption Coefficient (α)

Figure (4.18) shows how the absorption coefficient decreases at high wavelength and low energy, indicating that there is little likelihood of an electron transition taking place since the incident photon's energy is inadequately to transport the electron from the valence band to the conduction band. The absorption coefficient is measured in cm^{-1}. As in the equation (2.10).

Given that absorption is good at these energies, which suggests that there is a high likelihood for electron transitions, the energy of the incedent photon is adequate to shift the electron from the valence band to the conduction band at high energies [103,104]. This shows that the absorption coefficient assists in figuring out the nature of electron transition, when the values of the absorption coefficient are high ($\alpha > 10^4$)cm^{-1} at high energies it is expected that direct transition of electron occur, the energy and moment are maintained by the electrons and photons. While, when the values of the absorption coefficient is low ($\alpha < 10^4$) cm^{-1} at low energies, it is expected that indirect transition of electron occur, and the electronic momentum is maintained with the assistance of the phonon [83]. Among other results is that the absorption of coefficient for the (UHMWPEO/Cu/Ag-SiO_2) nancomposites is less than (10^4) cm^{-1}, this indicates that the electron transitions is indirect. We notice an increase in the absorption coefficient when adding silica nanoparticle.

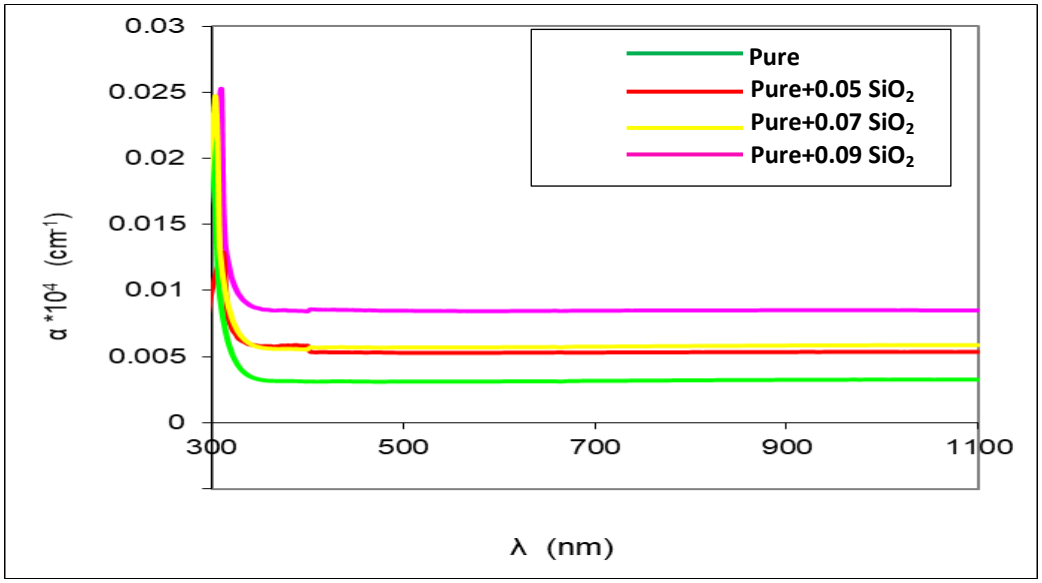

Fig. (4.18): Variation of Absorption Coefficient of (UHMWPEO/Cu/Ag-SiO_2).

4.3.5 Refractive Index (n)

This physical phenomenon, which frequently results in the exponential decay of light intensity as it travels, causes the rate of absorption of light to be directly proportional to the intensity of the incident light at a particular wavelength refractive index can be expressed by the following equation (2.14).

The variation in refraction index of (UHMWPEO/Cu/Ag-SiO_2) nanocomposites as a function of wavelength is shown in Figure (4.19). The statistics clearly show that when the weight proportion of (SiO_2) nanoparticles in the composite increases, the refractive index rises due to the increased density of the nanocomposites. We observe high refractive index values in the UV range due to its low transmittance, whereas we observe low values in the visible region due to its high transmittance [105].

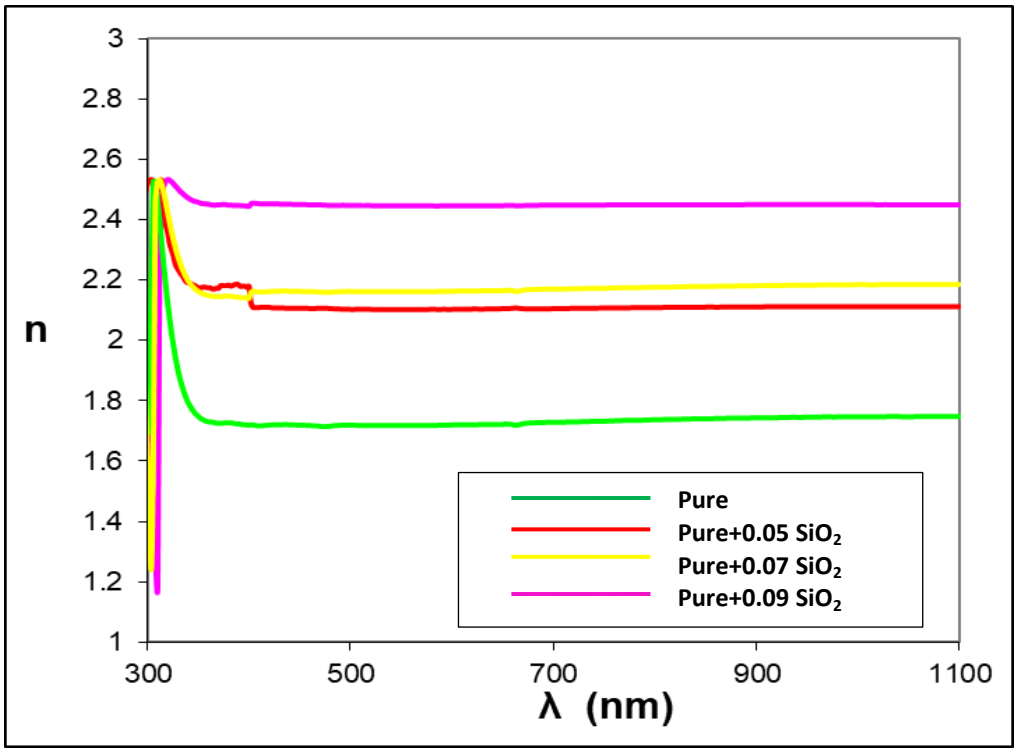

Fig. (4.19): Variation of Refractive Index for (UHMWPEO/Cu/Ag-SiO_2).

An increase in the refractive index means that the optical density has become greater, and this indicates an increase in the refractive ray with an increase in the addition of silica nanoparticles.

4.3.6 Extinction Coefficient (k_o)

Figure (4.20) shows that (k_o) decreases in value at low concentrations, but increases as (SiO_2) nanoparticle concentration increases. This is explained by an increase in the absorbance coefficient with (SiO_2) nanoparticle content. This finding suggests that the host material's structure will change as a result of the (SiO_2) nanoparticles [106]. The extinction coefficient is expressed in the following relationship(2.15).

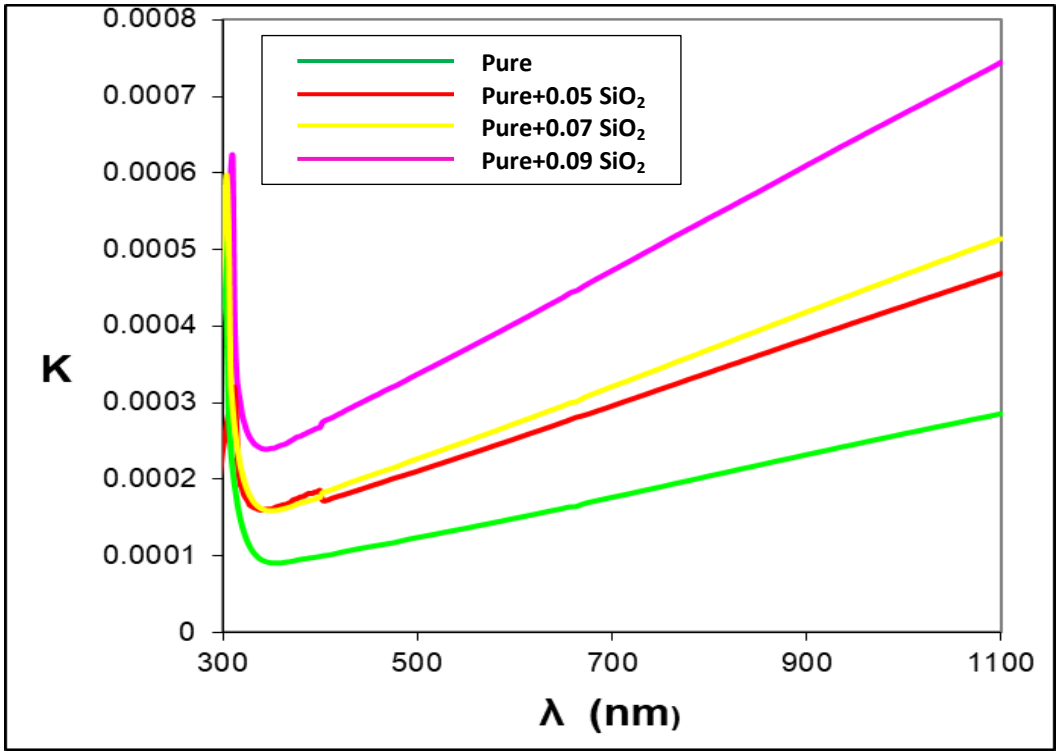

Fig. (4.20): Variation of Extinction Coefficient of (UHMWPEO/Cu/Ag-SiO_2).

4.3.7 Indirect Energy Gap

Figure (4.21) shows the relationship between edge absorption $(\alpha h\nu)^{1/2}$ of (PEO/Cu/Ag-SiO_2) nanocomposites as a function of photon energy, when drawing a straight line from the top of the curve towards the (x) axis at $(\alpha h\nu)^{1/2} = 0$ extrapolation, we get the energy gap of the permissible indirect transition. The obtained values are shown in table (4.9).

After adding silica nanoparticles to the superimposed, new levels were formed between the levels of the superimposed, which led to the convergence of the valence band and conduction bands from each other directly with the increase of silica particles, which indicates that the values of the energy gap decrease with the increase of the weight ratios of the nanoparticles, and this is due to the formation of local levels in the energy gap forbidden [107].

The transition in this case takes place in two stages that includes the transition of the electron from the valence band to the local levels to the conduction band as a result of increasing the weight ratio of nanoparticles.

The density of the state increased with the increase in the concentration of nanoparticles, which explains the decrease in the energy gap with the increase of nanoparticles as shown in Figure (4.21) and table (4.9) these results are similar to the researchers [107].

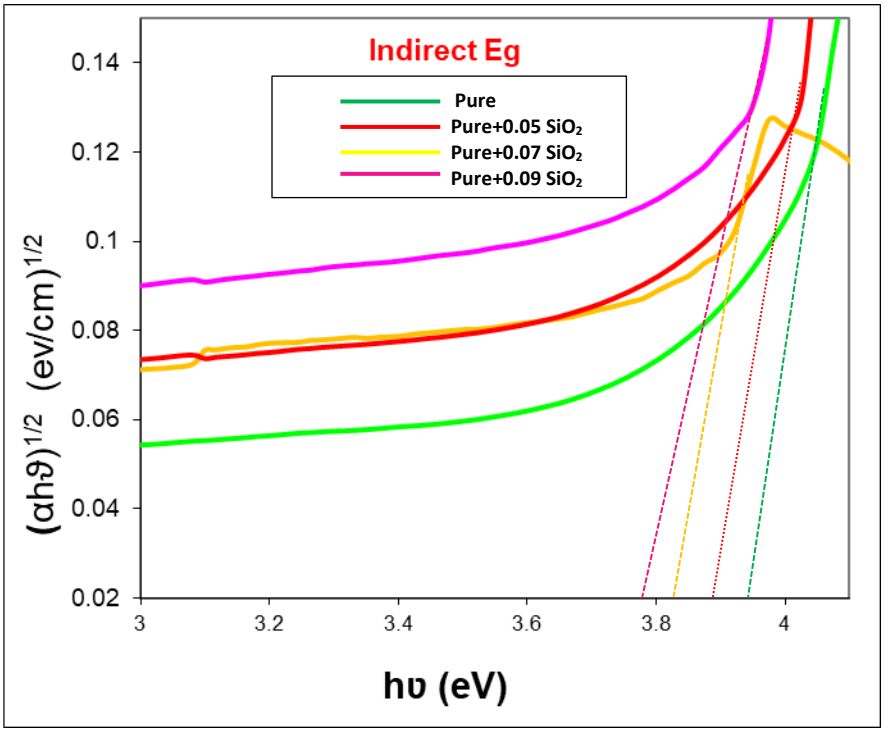

Fig. (4.21): Variation of Energy Gaps of (UHMWPEO/Cu/Ag-SiO_2).

Table (4.9): Energy Gaps Value of (UHMWPEO/Cu/Ag-SiO_2)

Sample	Indirect Eg(eV)
UHMWPEO/Cu/Ag	3.95
UHMWPEO/Cu/Ag+ 0.05 SiO_2	3.90
UHMWPEO/Cu/Ag+ 0.07 SiO_2	3.84
UHMWPEO/Cu/Ag+ 0.09 SiO_2	3.78

4.4 Conclusions

The following remarks are concluded during the present work:

1- In the study, we successfully prepared and investigated UHMWPEO/ Cu/ Ag films with out and within SiO_2 in the thicknesses about (75-85) μm.
2- No chemical interaction was appear after incorporation of SiO_2.
3- The purity of all materials was confirmed using (EDX) analysis.
4- According to the FESEM results, the images show fine diffusion, which may indicate that the nanoparticles are well dispersed within the UHMWPEO matrix. This is an important property of composite materials, as it can affect their properties. The statement also indicates that the images reveal several shapes that appeared in the composite material, which may mean that the nanoparticles formed in distinct structures or patterns, including floral, spherical, and other shapes, as well as an increase in the granular size, as it starts from (35.7)nm without silica, and the granular size increases with increasing concentrations of silica nanoparticles up to (54.2)nm.
5- X-ray diffraction examinations showed an increase in the crystal size of the UHMWPEO / Cu / Ag films, where it was found that the crystal size was (30.06) nm for the composite without silica, but it began to increase with the increase. in weight ratios of SiO_2 (37.12) nm
6- It was found that by studying the optical properties of the superimposed a clear improvement, through increasing the absorbance, reflectivity and optical coefficients with increasing the percentage of the weight concentration of silica, as for the transmittance and the energy gap, they decrease with the increase in the weight path, as the energy gap is less than (3.95)eV for the superimposed without silica particles until up to (3.78)eV with a concentration of (0.09)wt% of SiO_2 NPs.

7- The outcomes films make these nanocomposites suitable for using in the optoelectronic devices, solar cells, UV-detectors and etc.

4.5 Future Works

From this study, other future works can be adopted as suggested below:

1- Study of the structural and optical properties of films (UHMWPEO/ CuNPs/ AgNPs/ SiO_2) prepared by another method such as spin coating method.
2- Study the thermal and mechanical properties of (UHMWPEO/ CuNPs/ AgNPs/ SiO_2) nanocomposites.
3- Effect of irradiation on the electrical and optical properties of (UHMWPEO /CuNPs / AgNPs / SiO_2) nanocomposites.
4- Effect of temperature on the A.C. electrical properties of (UHMWPEO /CuNPs /AgNPs /SiO_2) nanocomposites.

.

References

[1] Mouritz A. and Gibson A., "Fire Properties of Polymer Composite Materials", Solid Mechanics and Its Applications, Vol. 143, pp.1-18, (2007).

[2] Asogwa P., "Effect of Deposition Medium on the Optical and Solid State Properties of Annealed MnO_2 Thin Films", J. of Optoelectronics and Biomedical Materials, Vol. 2, pp.109-117, (2010).

[3]Mark J., "Physical Properties of Polymers Handbook", Springe, Vol. 107, p.825, (2007).

[4] Logothetidis S., "Nanostructured Materials and Their Applications", Springer, pp.1-23, (2012).

[5] Köhler M. and Fritzsche W., "Nanotechnology an Introduction to Nano Structuring Techniques", Wiley, Vol.2, (2008).

[6] Bell A. , "The Impact of Nanoscience on Heterogeneous Catalysis", Sci., Vol. 299, No. 5613, pp.1688-1691, (2003).

[7] Shenoy K., "Effects of Multi-Wall Carbon Nanotubes on the Mechanical Properties of Polymeric Nanocomposites", M.Sc. Thesis, Department of Mechanical Engineering and the Faculty of the Graduate School of Wichita State University, (2008).

[8] Mustafa S., "Engineering Chemistry", Library of Arab Society for Puband Dis. Jordan, (2008).

[9] Long A. and Clifford M., "Composite Forming Mechanisms and Materials Characterization", Composites Forming Technologies, pp.1-21, (2007).

[10] Muheisin A., "Study of Electrical Conductivity for Amorphous and Semi Crystalline Polymers Filled with Lithium Fluoride Additive", M. Sc. Thesis, University of Mustansiriah, College of Science, (2009).

[11] Schultz J. M., "Polymer Materials Science", Prentice Hall, p.363, (1974).

References

[12] Kolahalam L., Kasi V., Diwakar B., Govindh B., Reddy V. and Murthy Y., "Review on Nanomaterials, Synthesis and Applications", Mater Today Proc, Vol. 18, No. 6, pp. 2182-2190, (2019)

[13] Kim S., Kim J. and Kim H., "Deposition of MgO Thin Films by Modified Electrostatic Spray Pyrolysis Method" ,Journal of Thin Solid Films ,Vol.376, pp. 110-114, (2000).

[14] Thanachayanont C., Yordsri V. and Boothroyd C.,"Microstructural Investigation and SnO Nanodefects in Spray-Pyrolyzed SnO_2 Thin Films", Journal of Materials Letters, Vol. 65, pp. 2610–2613, (2011).

[15] Sarathchandran C. , Devika M., Swetha P. and Sujatha S. , "Synthesis, Properties and Applications", Handbook of Carbon-Based Nanomaterials, , pp. 783-827, (2021).

[16] Stober A. and Bohn J., "Controlled Growth of Monodisperse Silica in the Micron Size Range", Journal Coll. Int. Sci, Vol. 26, p. 62, (1968).

[17]Bogush G. and Zukoski C. "Preparation of Monodisperse Silica Particles: Control of Size and Mass Fraction", Journal Non-Cryst. Sol. Vol. 104, pp. 95-105, (1988).

[18]Kim S., Kim H., Kim S. and Kim W., "Effect of Electrolyte Additives on Sol Precipitated Nano Silica Particles", Ceramics International Vol. 30, p.171,(2004).

[19]Rahman I., Vejayakumaran P. and Chee C., "Effect of Anion Electrolytes on the Formation of Silica Nanoparticles the Sol–gel Process" ,Ceramics International Vol. 32, p. 691, (2006).

[20] Jenkins A., "Polymer Science: A Material Science", Handbook, North Holland, Vol.2 , p. 912, (2013).

[21] Hsu P., Wu H. and Carney J., "Passivation ,Coating on Electrospun Copper Nanofibers for Stable Transparent Electrodes", ACS Nano, Vol. 6,No.6 ,pp. 5150-5156, (2012).

References

[22] Lin B., Gelves G. , and Haber J., "Electrical, Morphological and Rheological Study of Melt-Mixed Polystyrene/Copper Nanowire Nanocomposites", Macromolecular Materials and Engineering, Vol.293, No.7, pp. 631-640, (2008).

[23] Jung S., Preston D. and Jung H ., "Porous Cu nanowire Aero Sponges from One-Step Assembly and their Applications in Heat Dissipation", Advanced Materials, Vol.28, No.7, pp.1413-1419, (2016).

[24] Lee J., Park J., Kim M., Chang T., Kim S., Koo S. and Lee S., "Silver Complex Inks for Ink-jet Printing: the Synthesis and Conversion to a Metallic Particulate Ink", Journal of Ceramic Processing Research, Vol. 8, No.3, p. 219, (2007).

[25] Dankovich A. and Gray D., "Bactericidal Paper Impregnated with Silver Nano Particles for Point-of-Use Water Treatment", Materials Science, Vol. 45, No.5, (2011).

[26] Abou E., Etihad A. and Al-Waltham A., "Synthesis and Application of Silver Nanoparticles", Journal of Chemistry, Vol. 3, pp. 135-140, (2010).

[27] Herman F., "Encyclopedia of Polymer Science and Technology", John Wiley and Sons Inc., Vol. 14, New York, (1971).

[28] Karar A., "Enhancement of Some Physical Properties of Polyethylene Glycol by Adding Some Polymeric Cellulose Derivatives and its Applications" Ph. D Thesis, University of Babylon, College of Science,Department of Physics , (2015).

[29]- Banerjee S., Khamrai M., Sarkar K., Singha N. and Kundu P., "Modified Chitosan Encapsulated Core-Shell Ag Nps for Superior Antimicrobial and Anticancer Activity", International journal of biological macromolecules, Vol. 85, pp. 157-167, (2016).

[30] Ningning Z., Shuguang F., Jingyi M., Yujuan Z., Shengmao Z., Pingyu Z. and Zhijun Z., "Synthesis and Application of Copper Nanowires and Silver Nano sheet-Coated Copper Nanowires as Nano Fillers in Several Polymers" Nanowires, Condensed Matter Physics, DOI: 10.5772/67782, (2017).

References

[31]Bangyao H., Fenglian S., Yang L., Tianhui L. and Shushui P. , "Effect of Cu, Ag on the Microstructure and IMC Evolution of Sn_5Sb–CuAgNi/Cu Solder Joints", Materials Research Express, Vol. 6, No. 8, (2019).

[32]Shujahadeen B., Rawezh B., Amir N. , Hiwa A. and Younis A. " Structural, Thermal, Morphological and Optical Properties of PEO Filled with Biosynthesized Ag Nanoparticles: New Insights to Band Gap Study", Results in Physics, Vol. 13 ,p. 10222 ,(2019).

[33] Ragab H. and Rajeh A., "Structural, Thermal, Optical and Conductive Properties of PAM/PVAPolymer Composite Doped with Ag Nanoparticles for Electrochemical Application", J. Mater. Sci. Mater. Electron, Vol. 31, No. 19, pp.16780–16792, (2020).

[34] Karaar A.O. and Kalid. H.A. , "Effect of Silver Nano-Particles on Structural, Optical and Electrical Properties of Casted (Polyvinyl alcohol / Polyacrylamide / Polyethylene Oxide) Composites for Antibacterial Applications", DOI:10.21203/rs.3.rs-324880/v1, (2021).

[35] Han Q. , Yan L. , Xiaopeng L. , Di M. , Qianqian C. and Tao Z., "Fabrication of Ag Containing Antibacterial PEO Coatings on Pure Mg", Materials Letters, Vol.293, No.15, (2021).

[36] Xinzhen F., L'Hocine Y. and Edward S., "Antimicrobial Properties of the Ag, Cu Nanoparticle System", Biology, Vol.10, No.2, p.137, (2021).

[37] Ahed A.K., "Synthesis and Characterization of PAAm-PEG Blend and the Effect of Ag, Sb_2O_3 Nanoparticles: Structural and Dispersion Parameters", M. sc. Thesis, University of Babylon, College of Science, physics Department,(2022).

[38] Zainab M., "Effect of Nanowire on Structural and Optical Properties PVA-PAAm Blend", M. sc. Thesis University of Babylon, College of Education for Pure Sciencecs, Physics Department,(2022).

References

[39] Tian W., Guo L., Wang Y., Zhou P. and Zhang T., "Effect of Cu-/Ag-Activation on Growth and Corrosion Resistance of Electroless Plated Ni-Film on Plasma Electrolytic Oxidation Coating" , Journal of Chinese Society for Corrosion and protection, Vol. 42, No.4, pp. 573-582, (2022).

[40] Karar A., Khalid H., Ehssan A., Enas M. and Ashraq M., "Morphological, Optical, Electrical Characterizations and Anti-escherichia Coli Bacterial Efficiency (AECBE) of PVA/PAAm/PEO Polymer Blend Doped with Silver NPs", Nano Biomed. Eng., Vol. 14,No.8, (2022).

[41] Ehssan A., Ali T., Hikmat A. , Karar A. and Mohammed M. , "Effect of Green Synthesis Bimetallic Ag@SiO_2 Core–Shell Nanoparticles on Absorption Behavior and Electrical Properties of PVA PEO Nanocomposites for Optoelectronic Applications", Silicon, (2023).

[42] Camillo L. and Gianfranco R., "Polymer Wrapping Onto nanoparticles Induces the Formation of Hybrid Colloids", Coatings , Vol.13, No.5, (2023).

[43] Daniel M. and Astruc D., "Gold Nanoparticles: Assembly, Supramolecular Chemistry, Quantum-Size-Related Properties, and Applications toWard Biology, Catalysis, and Nanotechnology", Chemical Reviews, Vol.104, pp.293-346, (2004).

[44] Ragab H. , "Spectroscopic Investigations and Electrical Properties of PVA/PVP Blend Filled with Different Concentrations of Nickel Chloride", Journal Physical, Vol.406, No.20, pp.3759–3767, (2011).

[45] Karar A., " Structural, Optical, Electrical Properties, and Relative Humidity Sensor Application of PVA/Dextrin Polymeric Blend Loaded with Silicon Dioxide Nanoparticles", Journal of Materials Science: Materials in Electronics. Vol. 33, pp.18199–18208, (2022).

[46] Theophanides T., "Introduction to Infrared Spectroscopy", Infrared Spectroscopy-Materials Science, Engineering and Technology, pp. 1-10, (2012).

References

[47] Baogang Z., Chuanping F., Jinren N. and Jing Z., "Simultaneous Reduction of Vanadium (V) and Chromium (VI) with Enhanced Energy Recovery Based on Microbial Fuel Cell Technology", The International Journal, b, pp. 34-39, (2012).

[48] Abdelrazek E. , Abdelghany M., Badr A. and Morsi, M.,"Structural, Optical, Morphological and Thermal Properties of PEO/PVP Blend Containing Different Concentrations of Biosynthesized Au Nanoparticles", Journal of Materials Research and Technology, Vol.7,pp. 419-431, (2018).

[49] Abdelrazek E., El Damrawi G., Elashmawi I. and El-Shahawy, A., "The Influence of Y-irradiation on Some Physical Properties of Chlorophyll/PMMA Films", Applied Surface Science, Vol.256, pp.2711-2718. (2010).

[50] Eissa M., Kaid M. and Kamel N., "The Influence of Low-and High-Linear Energy Transfers on Some Physical Properties of Poly (Methyl-Methacrylate) Samples", Journal of Applied Polymer Science, Vol.125, pp. 3682-3687, (2012).

[51] Khursheed A., "Scanning Electron Microscope Optics and Spectrometers, Scanning Electron Microscope Optics and Spectrometers", World scientific, pp. 1– 403, (2010).

[52] Lyman C., Newbury D., Goldstein J., Williams D., Romig A., Armstrong J., Echlin P., Fiori C., Joy D., Lifshin E. and Peters K., "Scanning Electron Microscopy, X-Ray Microanalysis and Analytical Electron Microscopy: A Laboratory Workbook, Plenum Press", New York, pp. 180-186, (1990).

[53] Essner J., and Baker G., " The Emerging Roles of Carbon Dots in Solar Photovoltaics" , Environmental Science: Nano, Vol.4, pp.1201- 1420,(2017).

[54] Cullity B., "Lements of X-Ray Diffraction", Addison-Wesley, Publishing Company, ISBN 0-201-01174-3, (1970).

[55] Quinn J. and Yi K. S., " Solid State Physics Principles and Modern Applications", Springer-Verlag Berlin Heidelberg,Vol.6, No.94, p.17, (2009).

References

[56] Anna C ., Todd E. and Thomas P., " Nanoparticle Polymer Composites: Where two Small Worlds Meet", Science, DOI: 10.1126/science.1130557,(2006).

[57] Hashim A., Rabee B., Habeeb M., Abd-alkadhim N. and Saad A., "Study of Electrical Properties of (PVA-CaO) Composites", American Journal of Scientific Research, Vol. 73, pp. 5-8, (2012).

[58] Vangindertael R., Camacho' W., Sempels H. Mizuno P. Dedecker K and Janssen K., "An Introduction to Optical Super-Resolution Microscopy for the Adventurous Biologist", Methods and Applications in Fluorescence, Vol.6, No.2, (2018).

[59] Abdulmitalib A."Studying in Electric and Optical Properties of Polymers with Application on Non Crystal Films from Poly Acrylic Acid", M. Sc. Thesis, College of Science, University of Basrah, (1981).

[60] Raheem G. and Ahmed S., "Study of Optical Properties of (PEO-PEG) Blends", Journal University of Kerbala, Vol. 12, No. 2, pp.163-174, (2016).

[61] Cheong K., "Review on Oxides of Antimony Nanoparticles: Synthesis, Properties, and Applications", Journal of Materials Science, Vol. 45, No. 22, (2010).

[62] Nalwa H., "Handbook of Surfaces and Interfaces of Materials", Elsevier, Vol.5, (2001).

[63] Rabee B., Razooqi F. and Shinen M., "Investigation of Optical Properties for (PVA-PEG-Ag) Polymer Nanocomposites Films", Chem. Mater. Res., Vol. 7, No.4, pp. 103-109, (2015).

[64] Pankove J. I., "Optical Processes on Semiconductors Dover Publication", Inc. New york, (1971).

[65] Donald A., "Semiconductor Physics and Devices", Basic Principles , Vol. 247, (1992).

References

[66] Suryawanshi V., Varpe A. and Deshpande M., "Band Gap Engineering in PbO Nanostructured Thin Films by Mn Doping", Thin Solid Films, Vol. 645, pp. 87-92, (2018).

[67] Nahida J., "Spectrophotometric Analysis for the UV-irradiated (PMMA)", International Journal of Basic and Applied Sciences, Vol.12, No.2, pp. 58-67, (2012).

[68] Obaid Z. "Physical Properties of PMMA/ZnO Composite Material", Diss. Ministry of Higher Education, (2017).

[69] Chuang S., "Optical Processes in Semiconductors", Physics of Photonic Devices, 2nd ed.; Boreman, G., pp. 347-389, (2009).

[70] Jenkins F. and White H., "Fundamentals of Optics", Indian Journal of Physics, Vol. 25, pp. 265-266, (1957).

[71] Berglund R., Graham P. and Miller R., "Applications of In-situ FT-IR in Pharmaceutical Process R and D", spectroscopy-Springfield then Eugene-, Vol. 8, p.31,(1993).

[72] Suganthi S., Vignesh S., Sundar J. and Raj V., "Fabrication of PVA Polymer Films With Improved Antibacterial Activity by Fine-tuning Via Organic Acids for Food Packaging Applications", Applied Water Science, Vol. 10, No.4, pp.1-11,(2020).

[73] Goldstein J., Newbury D., Echlin P., Joy D., Lyman C., Lifshin E., Linda S. and Michael J., "Scanning Electron Microscopy and X-Ray Microanalysis", Kluwer Academic, New York, (2003).

[74] Di Marco G., Lanza M., Pennisi A. and Simone F., "Solid State Electrochromic Device: Behaviour of Different Salts on its Performance", Solid State Ionics, Vol.127, pp. 23-29, (2000).

References

[75] Abdali K., Al-Bermany E. and Abass K., "Impact the Silver Nanoparticles on Properties of new Fabricated Polyvinyl Alcohol- Polyacrylamide- Polyacrylic Acid Nanocomposites Films for Optoelectronics and Radiation Pollution Applications", Journal of Polymer Research. Vol.30, No.138, (2023).

[76] El-naggar A., Heiba Z. ,Mohamed M. and Kamal A. , "Effect of Nano CdS/Mg on Linear and Nonlinear Optical Characteristic of PVA/PVP/PEG Film", Journal of Materials Science, Vol.33, No. 21, pp.17235-17248, (2022).

[77] Yakuphanoglu F. and Erten H., "Refractive Index Dispersion and Analysis of the Optical Constants of an Ionomer Thin Film", Optica applicata, Vol. 35, No. 4, pp. 969–976, (2005).

[78] Verma P., Sardar P., Ghosh S. and Biswas M., "Conducting Nanocomposites of Polyacrylamide with Acetylene Black and Polyaniline", Polymer composites, Vol.30,No. 4, pp.490-496,(2009).

[79] Yakovenko O., Matzui L. , Vovchenko L. , Oliynyk V. and Trukhanov A., "Dielectric Properties of Composite Materials Containing ligned Carbon Nanotubes", Inorganic Materials, Vol. 52, No. 11, pp.1198-1203, (2016).

[80] Al-Khalaf A., Abdali K., Mousa A. and Zghair M. "Preparation and Structural Properties of Liquid Crystalline Materials and its Transition Metals Complexes", Asian Journal of Chemistry, Vol.30, No.2, (2019).

[81] Chichan O., Rasheed K., Saleh A., Chiad S., and Habubi N. , "Synthesize of CdS and CdS: V Films via Spray Pyrolysis Technique: Morphology and Optical Properties", Design Engineering, pp.356-365, (2021).

[82] Tuama A., Abbas K., Hamzah M., Mezan S., Jabbar A. and Agam M., "An Overview on Characterization of Silver/Cuprous Oxide Nanometallic (Ag/Cu_2O) as Visible Light Photocatalytic", International Journal of Advanced Science and Technology, Vol.29, No. 3, pp.5008-5018, (2020).

References

[83] Necula B. , Tichelaar F. and Duszczyk J., "An Electron Microscopical Study on the Growth of TiO_2–Ag Antibacterial Coatings on Ti6Al7Nb Biomedical Alloy", Acta Biomaterialia, Vol. 7, No. 6, pp. 2751-2757, (2011).

[84] Lu G., Anderson B., Grondelle R. , Santen W. and Gennip H., "Alumina-Supported Cu–Ag Catalysts for Ammonia Oxidation to Nitrogen at Low Temperature", Journal of Catalysis, Vol. 206, No. 1 , pp.60-70 ,(2011)

[85] Morán D., Gutiérrez G., Blanco-López M., Marefati A., Rayner M. and Matos M., "Synthesis of Starch Nanoparticles and their Applications for Bioactive Compound Encapsulation", Applied Sciences, Vol. 11, No. 10, (2021).

[86] Dularia C., Sinhmar A., Thory R., Pathera A. and Nain V., "Development of Starch Nanoparticles Based Composite Films from Non-conventional Source-Water Chestnut (Trapa bispinosa)", International journal of Biological Macromolecules, Vol.136, pp.1161-1168, (2019).

[87] Campelo P., Sant'Ana A. and Clerici M. , "Starch Nanoparticles: Production Methods, Structure, and Properties for Food Applications", Current Opinion in Food Science, Vol.33, pp.136-140, (2020).

[88] Safa A., Sarah M., Ali R., Ehssan A. and Karar A., "AC Conductivity, and Optical Characterizations of (PVA-PEG) Doped SrO Hybrid Nanocomposites", Key Engineering Materials, Vol.936, pp.83-92, (2022).

[89] Mahdi A., Abbass R. and Abd G., "Investigation of SiO_2 and FO Oxidation Mechanisms by Carbon and Boron Nitride as Acceptable Nano-catalysts", Silicon, Vo.15, No.6, (2023).

[90] Abdelamir A., Al-Bermany E. and Hashim F., "Important Factors Affecting the Microstructure and Mechanical Properties of PEG/GO-Based Nanographene Composites Fabricated Applying Assembly-Acoustic Method", In AIP Conference Proceedings, Vol. 2213, No. 1, p. 020110, (2020).

References

[91] Elmetwally M., Abdelrazek a b Amr M., Shalabya I., Badr b., Mohamed A. and Morsi d., "Tructural, Optical, Morphological and Thermal Properties of PEO/PVP Blend Containing Different Concentrations of Biosynthesized Au Nanoparticles", Journal of Materials Research and Technology, Vol.7, No.4, pp. 419-431,(2018).

[92] Anran G., Martina R., Paolo C., Jiachen L. and Michele M., "In Situ Carbon Thermal Reduction Method for the Production of Electrospun Metal/SiOC Composite Fibers", Journal of Materials Science, Vol.50, pp.2735–2746, (2015).

[93] Su-Su H., Li L., Li-Ping M., Jia-Ying Z., Fei-Y., Ai-Jun W. and Jiu-Ju F., "Electrochemical Sensor for Nitrite using a Glassy Carbon Electrode Modified with Gold-Copper Nanochain Networks", Springer, Vol.183, pp.791–797, (2016).

[94] Aldulaimi N. and Al-Bermany E., "Tuning the Band Gap and Absorption Behaviour of the Newly-fabricated Ultrahigh Molecular Weight Polyethylene Oxide- Polyvinyl Alcohol/ Graphene Oxide Hybrid Nanocomposites", Polymer and Polymer Composite , Vol.30, No.4, pp.1-14,(2022).

[95] Ramiro G. , Alexis M., Luis M., Jason G. and Mataz A., "Forcespun Poly Vinyl Pyrrolidone /Copper and Polyethylene Oxide/Copper Composite Fibers and Their use as Antibacterial Agents" Applied Polymer, Vol.139, No.11, (2022).

[96] Karar A., "Structural, Morphological, and Gamma Ray Shielding (GRS) Characterization of HVCMC/PVP/PEG Polymer Blend Encapsulated with Silicon Dioxide Nanoparticles", Silicon. Vol.14, pp.9111-9116, (2022) .

[97] Hasan M ., Ramiro G., Munoz A., Luis M., Jason G. and Mataz A., "Forcespun polyvinylpyrrolidone/copper and polyethylene oxide/copper composite fibers and their use as antibacterial agents", Applied Polymer Science, Vol.193, No.11, (2022).

[98] Karar A., "Novel Flexible Glass Composite Film for Stretchable Devices Applications", Silicon, Vol.15, No.6, (2023).

References

[99] Mukheef S., Hashim F. and Abass K, "Fabrication and Investigation of the Structural, Morphological and Optical Properties of Iron Oxide by Thermal Evaporation Technique and Antibacterial Applications", HIV Nursing, Vol.22, No.2, pp.849–854, (2022).

[100] Cyriac V., Noor I. , Mishra K., Chavan C., Bhajantri R. and Masti S. , "Ionic Conductivity Enhancement of PVA: Carboxymethyl Cellulose Poly-blend Electrolyte Films Through the Doping of NaI Salt", Cellulose, Vol.29 No.6, pp.3271-3291, (2022).

[101] Anwar A., Fadhl A., Karar A. and Abdulazees O., "Effect of Molar Concentration and Solvent Type on Linear and NLO Properties of Aurintricarboxylic (ATA) Organic Dye for Image Sensor and Optical Limiter Applications", International Journal of Nanoscience, Vol.22, No.2, (2023).

[102] Al-Zuhairi A., Allw A., Abdali K., Rasool S. and Mousa A., "Synthesis of Hyperbranched Polymers and Study of its Optical Properties", J. of Engineering and Applied Sci. Vol.12, No.6, pp.7800–7804, (2017).

[103] Karar A., Lamis F., Alhak A., Abdulazeez O. and Ali A., "Enhancing Some Physical Properties of Cosmetic Face Powders", Journal of Global Pharma Technology, Vol.10, pp. 75-78, (2018).

[104] Abdali K., "Synthesis, Characterization and USW Sensor of PEO/PMMA/PVP Doped with Zirconium Dioxide Nanoparticles", Transactions on Electrical and Electronic Materials, Vol. 23 . No. 5, pp. 563-568, (2022).

[105] Sivakumar M., Subadevi R., Rajendran S., Wu N. and Lee J. , "Electrochemical Studies on [(1− x) PVA–xPMMA] Solid Polymer Blend Electrolytes Complexed with $LiBF_4$", Materials Chemistry and Physics, Vol. 97,No.2 ,pp.330-336, (2006).

[106] Nakamura Y., Kariya E., Fukuda T., Fujii S., Fujiwara K. and Hikasa S., "Glass Transition Behaviour of PMMA/PVA Incompatible Blend", Polymers and Polymer Composites, Vol. 21,No.6 ,pp. 367-376, (2013).

References

[107] Yang J., Yan X., Wu M., Chen F., Fei Z. and Zhong, M., "Self-Assembly Between Graphene Sheets and Cationic Poly (Methyl Methacrylate)(PMMA) Particles: Preparation and Characterization of PMMA/Graphene Composites", Journal of Nanoparticle Research, Vol.14, No.1, pp.1-9, (2012).

List of Contents

List of Figures

List of Tables

List of Symbols and Abbreviations

Symbol	Description	Unit
UHMWPEO	Ultra High Molecular Weight Poly Ethylene Oxide	-
CuNPs	Copper Nanoparticles	nm
AgNPs	Silver Nanoparticles	nm
SiO_2	Silicon Dioxide	nm
TEOS	Tetraethyl Ortho Silica	-
T	Transmittance	-
A	Absorption	-
hυ	Photon Energy	J
h	Planks Constant	J.s
α	Absorption Coefficient	cm^{-1}
k_o	Extinction Coefficient	-
I_o	Photon Beam Intensity	-
I_t	Intensity of Light Transmitted	-
t	Thickness	µm
n	Refractive Index	-
d	Density	g/cm^3
c	Light Speed in Vacuum	m/s
v	Light Speed in Matter	m/s
R	Reflectance	-
σ_{op}	Optical Conductivity	s^{-1}
λ	Wavelength	nm
E_g	Energy Gap	eV

Symbol	Description	Unit
D	Distance	M
L.R.O.	Long Range Order	-
S.R.O.	Short Range Order	-
V	Volume	m^3
UV-VIS	Ultraviolet-Visible Spectrophotometer	-
FTIR	Fourier Transforms Infrared	-
EDX	Energy Dispersive X-ray Spectroscopy	-
FESEM	Field Emission Scanning Electron Microscopy	-
XRD	X-ray Diffraction	-
$\boldsymbol{\varepsilon_1}$	Real Part	-
$\boldsymbol{\varepsilon_2}$	Imaginary Part	-
T_g	Glass Transition Temperature	K
T_m	Melting Point Temperature	K
T_b	Boiling Point Temperature	K
α_{op}	Absorption Coefficient	-
LED	Light-Emitting Diode	-
APS	Actual Particle Size	nm